İZMİR KÂTİP ÇELEBİ ÜNİVERSİTESİ
2010
GRADUATE SCHOOL OF NATURAL AND APPLIED SCIENCES

Development of Nanoparticle Integrated Local Drug Delivery System for Tissue Regeneration

Submitted to the Graduate School of Natural and Applied Sciences in partial fulfillment of the requirements for the degree of

Master of Science

in Biomedical Engineering

by

Nursu ERDOĞAN

ORCID 0000-0003-3814-3480

July, 2021

This is to certify that we have read the thesis **Development of Nanoparticle Integrated Local Drug Delivery System for Tissue Regeneration** submitted by **Nursu ERDOĞAN** and it has been judged to be successful, in scope and in quality, at the defense exam and accepted by our jury as a MASTER'S THESIS.

APPROVED BY:

Advisor: **Assist. Prof. Dr. Didem ŞEN KARAMAN** ……..
İzmir Kâtip Çelebi University

Committee Members:

Prof. Dr. Berrin Tunca ……..
Bursa Uludağ University

Assoc. Prof. Dr. Nesrin HORZUM POLAT ……..
İzmir Kâtip Çelebi University

Assist. Prof. Dr. Didem ŞEN KARAMAN ……..
İzmir Kâtip Çelebi University

Date of Defense: July 02, 2021

Declaration of Authorship

I, **Nursu ERDOĞAN**, declare that this thesis titled **Development of Nanoparticle Integrated Local Drug Delivery System for Tissue Regeneration** and the work presented in it are my own. I confirm that:

- This work was done wholly or mainly while in candidature for the Master's degree at this university.
- Where any part of this thesis has previously been submitted for a degree or any other qualification at this university or any other institution, this has been clearly stated.
- Where I have consulted the published work of others, this is always clearly attributed.
- Where I have quoted from the work of others, the source is always given. This thesis is entirely my own work, with the exception of such quotations.
- I have acknowledged all major sources of assistance.
- Where the thesis is based on work done by myself jointly with others, I have made clear exactly what was done by others and what I have contributed myself.

Signature:

_____

Date: 09.07.2021

_____

Development of Nanoparticle Integrated Local Drug Delivery System for Tissue Regeneration

Abstract

There is an increasing concern that conventional drug delivery systems have disadvantages in the way of protective barriers, first-pass mechanism of human body, or characteristics of therapeutic agents. Local drug delivery systems can play an important role to overcome the challenges of conventional methods. However, the main challenge is the hydrophobic nature of therapeutic agents requires to develop novel designs. Nanofibers (NF) and nanoparticles are attractive in the field of drug delivery, especially for class IV therapeutic agents.

In this thesis, a local drug delivery system encompassing mesoporous silica nanoparticles (MSN) and poly ε-caprolactone (PCL) blended with methoxy poly(ethylene glycol) polyethyleneimine (mPEG: PEI) copolymer nanofibers was developed. The thesis aims to optimize PCL and mPEG: PEI blended nanofibers features and drug (i.e curcumin) loaded mesoporous silica nanoparticles then, determine drug release profile and tissue regeneration potential of curcumin loaded nanoparticles integrated nanofibers as a dura membrane. The study represents the enabling of nanofibers properties by varied blend composition and the drug release profile which is independent of polymer degradation. Designed nanofiber-based drug delivery system induces cell proliferation, viability and tissue regeneration with the accompanied curcumin loaded MSN and tuned mechanical support. To the best of our

knowledge, this thesis is the first study to suggest the integration of MSN and nanofibers by spin coating method as a local drug delivery system. The first step of the study is mPEG: PEI blended PCL nanofibers were fabricated by electrospinning then, mesoporous silica nanoparticles were synthesized by sol-gel method and curcumin was loaded into MSN as a model drug. In the next step, curcumin loaded MSN were accumulated onto nanofiber surfaces by spin coated method. Physicochemical characterizations were employed to predict the performance of the designed local drug delivery system as a dura graft material. Finally, drug release profile and cell attachment were determined to understand tissue regeneration potential. The obtained results revealed that accumulation of curcumin loaded MSN onto nanofibers surface by spin coating methods promoted cell proliferation. Moreover, a sustained drug release profile was obtained without polymer degradation and cell attachment studies showed that our design is promising as a synthetic graft.

Keywords: Local drug delivery systems, Nanofibers, Mesoporous silica nanoparticles, Dura membrane, Curcumin

Doku Yenilenmesi için Nanoparçacık Entegre Edilmiş Lokal İlaç İletim Sistemi Geliştirilmesi

Öz

Geleneksel ilaç iletim sistemlerinin; insan vücudundaki koruyucu bariyerler, ilk geçiş mekanizması veya terapötik ajanların özellikleri açısından dezavantajlara sahip olduğuna dair artan bir endişe vardır. Lokal ilaç iletim sistemleri, geleneksel yöntemlerin zorluklarının üstesinden gelmek için önemli bir rol oynayabilir. Buna rağmen başlıca sorun olan, terapötik ajanların hidrofobik doğası özgün tasarımların geliştirilmesini gerektirmektedir. Nanofiberler ve nanoparçacıklar ilaç iletim sistemi alanında özellikle sınıf 4 terapötik ajanlar için ilgi çekmektedir.

Bu tezde, mezoporöz silika nanoparçacıklar (MSN) ve metoksi polietilen glikol: polietilenimin (mPEG:PEI) kopolimeri karıştırılmış polikaprolakton (PCL) nanofiberlerini kapsayan bir lokal ilaç iletim sistemi hazırlanmıştır. Tezde, PCL ve mPEG:PEI karıştırılmış nanofiberlerin özelliklerinin ve ilaç (örneğin kurkumin) yüklü mezoporöz silika nanoparçacıkların optimizasyonlarının yapılması daha sonra ilaç salım profilinin ve kurkumin yüklü nanoparçacık entegre edilmiş nanofiberlerin dura zarı olarak doku rejenerasyon potansiyelinin belirlenmesi amaçlanmaktadır. Çalışmada, çeşitli karışım kompozisyonları ve polimer bozunmasından bağımsız olan ilaç salım profili ile nanoliflerin özelliklerinin etkinleştirilmesi sunulmuştur.

Tasarlanmış nanofiber bazlı ilaç iletim sistemi, beraberindeki kurkumin yüklü MSN ve ayarlanmış mekanik destek ile hücre çoğalmasını, canlılığını ve doku yenilenmesini indüklemektedir. Bilgimiz dahilinde bu tez, lokal ilaç iletim sistemi olarak MSN ve nanofiberlerin döndürmeli kaplama metodu ile entegre edilmesini gösteren ilk çalışmadır. Çalışmanın ilk adımı olan mPEG: PEI katkılanmış PCL nanofiberler elektroeğirme yöntemi ile üretilmiş, daha sonra mezoporöz silika nanoparçacıklar sol-jel metot ile sentezlenmiş ve model ilaç olarak kurkumin MSN içerisine yüklenmiştir. Bir sonraki aşamada kurkumin yüklü mezoporöz silika nanoparçacıklar nanofiber yüzeyinde döndürmeli kaplama metoduyla biriktirilmiştir. Tasarlanan lokal ilaç iletim sisteminin, dura yama malzemesi olarak performansının öngörülebilmesi için fizikokimyasal karakterizasyonları yapılmıştır. Son olarak, ilaç salım profili ve hücre tutunması doku rejenerasyon potansiyeli hakkında bilgi sahibi olmak için belirlenmiştir. Elde edilen sonuçlar, MSN yüklü kurkuminin, döndürmeli kaplama yöntemiyle nanoliflerin yüzeyine birikmesinin hücre çoğalmasını desteklediğini ortaya koymuştur. Ayrıca, polimer bozulması olmadan sürekli bir ilaç salım profili elde edilmiştir ve hücre tutunma çalışmaları, tasarımımızın sentetik bir yama olarak umut verici olduğunu göstermiştir.

Anahtar Kelimeler: Lokal ilaç iletim sistemleri, Nanolifler, Mezoporöz silika nanoparçaçıklar, Dura Zarı, Kurkumin

To my lovely family…

Acknowledgment

First and foremost, I would like to thank my advisor, Assist. Prof. Dr. Didem ŞEN KARAMAN who provided an opportunity to improve myself in her laboratory. I am greatly appreciate for her understanding, support, sincerity, perseverance and encouragement. I learned a lot from her during my master's degree not only academically but also about personal life. I consider myself very lucky that she has mentored me.

We would like to acknowledge IKCU- Plasma Medicine Laboratory for cooperation to use of plasma device and IKCU-Tissue Engineering and Regenerative Medicine Laboratory. I also would like to present many thanks to my labmates in NanoMED& BioMAT Lab especially Ayşenur PAMUKÇU for her friendship and support during my MSc studies. Additionally, I would like to thank my friends Ece DENİZ and Emre TEKGÖZ for being there for me when I need it.

I would like to express my deep appreciation to my family who supports me in every challenge and decision in my life. I am grateful for their confidence in me.

We would like to thank Assist. Prof. Dr. Gülşah EREL AKBABA for providing fibroblast cell line, research assistant Mazlum Unay for his help about MATLAB analyses, and IKCU- Organic Semiconductor Materials Application Laboratory for their assistance to operate spin coater.

Also, I would like to acknowledge The Scientific and Technological Research Council of Turkey (TUBITAK) for financially supporting me under 2210&2211-MSc/MA/PhD Scholarship Programs (2210-C National MSc/MA Scholarship Program in the Priority Fields in Science and Technology).

Also, IKCU-Coordination Office of Scientific Research Projects was acknowledged for their funding under projects 2020-ÖDL-MÜMF-0004 and 2019-TYL-FEBE-0010.

Table of Contents

List of Figures

List of Tables

List of Abbreviations

µg	Microgram
APIs	Active Pharmaceuticals Ingredients
APTES	Aminopropyl triethoxysilane
BBB	Blood brain barrier
BCNU;carmustine	N,N0-bis[2-chloroethyl]-N-nitrosourea
BET	Brunauer–Emmett–Teller
$CaCl_2$	Calcium chloride
CAP	Cold atmospheric plasma
cm	Centimeter
CNS	Central nervous system
CSF	Cerebrospinal fluid
DAPI	4′,6-diamidino-2-phenylindole
DDSs	Drug delivery systems
DLS	Dynamic light scattering
FITC	Fluorescein-5isothiocyanate
GBM	Glioblastoma multiforme
h	Hour
HEPES	4-(2-hydroxyethyl)-1-piperazineethanesulfonic acid
HMDI	Hexamethylene diisocyanate
KCl	Potassium chloride
kHz	Kilohertz

kV	Kilovolt
LBADSA	Low bond axisymmetric shape analysis
mg	Milligram
$MgSO_4$	Magnesium sulfate
mL	Milliliter
mM	Millimolar
mm	Millimeter
mPEG	Methoxy polyethylene glycol
mPEG: PEI	Poly(ethylene glycol): polyethyleneimine
MSN	Mesoporous silica nanoparticles
MSN-Cur	Mesoporous silica nanoparticles loaded with curcumin
MSN-F	FITC labeled mesoporous silica nanoparticles
MSN-F-PPI	FITC labeled and polypropylene imine grafted mesoporous silica nanoparticles
MTT	3-(4,5-Dimethylthiazol-2-yl)-2,5-diphenyltetrazolium bromide
Mw	Moleculer weight
NaCl	Sodium chloride
NaH_2PO_4	Sodium dihydrogen phosphate
$NaHCO_3$	Sodium hydrogen carbonate
NF	Nanofiber
nm	Nanometer
PCL	Poly ε-caprolactone
PDGF-BB	Platelet-derived growth factor-BB
PDI	Polydispersity index
PEI	Polyethylenimine
PLGA	Poly (lactic-co-glycolic acid)

PPI	Polypropylene imine
PVA	Poly vinyl alcohol
rpm	Revolutions per Minute
SEM	Scanning electron microscope
Silica	Silicon dioxide
TGA	Thermogravimetric analysis atmosphere
UV	Ultraviolet radiation
VEGF	Vascular endothelial growth factor
W/V	Weight/volume
W/W	Weight/weight
wt.	Weight

List of Symbols

°	Degree
℃	Degree Celsius
θ	Theta
ζ	Zeta

Chapter 1

1.1. Introduction

Systemic drug administrations that include oral delivery, intravenous, and intramuscular injections are employed as the conventional delivery of drugs. However, systemic administrations may lead to suboptimal drug concentrations at the lesion site and might require repeated or high drug dosage. Through systemic administration, drugs can pass various bio-physicochemical environments. Therefore, adverse effects could be observed. On the other hand, drugs might be enzymatically and hydrolytically degraded or exposed to by the first-pass mechanism by the liver before reaching the site of interest for the treatment. Moreover, biological barriers or protective layers such as the blood-brain barrier, intestinal barrier, stratum corneum, and capillary endothelial barrier reduce the permeability of drugs [1,2].

To overcome limitations of systemic administrations local drug delivery systems (DDSs) are needed. Local DDSs such as topical, intranasal and ophthalmic administrations enable drugs to expose directly at the diseased site. Local DDSs aim to have proper drug doses at the lesion site, lessen adverse effects and provide safety, increase selectivity, efficiency, and patient's compliance [1,3]. Moreover, DDSs are expected to meet the requirement of controlled delivery and stability under physiological environments [4].

Therefore, commercially local drug delivery products with various materials and active agents have been developed (Table 1.1). For instance, Periodontal Plus AB™ is a collagen fibril that contains tetracycline hydrochloride to treat periodontitis. It is biodegradable and releases tetracycline consistently in the local area. On the contrary, Actisite ® another local DDS for treatment of periodontitis is a non-degradable fiber that is placed onto the damaged area and needed to remove [5].

Table1.1: Commercially available local drug delivery products for periodontitis [5]

Active agent	Product	Description
Tetracycline fiber	Actisite® (25 % tetracycline HCl)	Nonresorbable fiber
	Periodontal Plus AB™	Resorbable fiber
	PerioCol-TC	Resorbable fiber
Chlorhexidine chip	PerioChip® (2.5 mg)	Biodegradable chip
	PerioCol-CG (2.5 mg)	Biodegradable chip
	Chlo-Site (1.5 % CHX)	Biodegradable gel
Doxycycline polymer	ATRIDOX® (10 %)	Biodegradable powder in syringe system
Minocycline	Dentomycin (2 %)	Biodegradable gel
	Periocline (2.1 %)	Biodegradable gel
	ARESTIN®	Biodegradable microspheres in syringe system
Metronidazole gel	Elyzol (25 %)	Biodegradable gel

Once the diseases that could have high benefit from the DDS could be counted as antibacterial and anticancer therapies. For instance, the current treatment of bone infection has required the removal of infected tissue and later on antibiotic administration intravenously. However, in the recent investigation of Padrão et al., they developed heparinized nanohydroxyapatite-collagen granules and loaded vancomycin to prevent biofilm formation. It has been shown that vancomycin could provide sustained release for 19 days which provided the prevention of Methicillin-resistant *S. aureus* growth. Also, granule structures were found proper for enhancing bone regeneration in terms of interconnected macroporosity. The study indicated a design of a promising local drug delivery system for antibiotics while assisting new bone formation at the infected area [6]. The cancer treatments have got benefits from local drug delivery systems. In the literature studies, intravenous administration of anticancer drug cisplatin has been presented as an inefficient accumulation of drugs at the tumor site to kill cancer cells in vitro. Because of possible adverse effects such as kidney damage, nausea, bone marrow suppression development of DDS to reduce side effects is direly needed to reach an adequate dose. For this purpose polyethylene glycol-based implants were designed to reduce the accumulation of cisplatin on healthy tissues and enhancement of anticancer effect for tumor growth [7].

Central nervous system (CNS) disorders are challenging in terms of drug delivery due to the presence of protective barriers[4]. The blood-brain barrier (BBB) regulates the homeostasis of the CNS and protects it by restricting the transportation of molecules,

toxins or pathogens between capillaries and CNS. BBB able to restrict molecules because of the tight junction between endothelial capillary cells as in figure 1.1, various receptors, enzymes, and alternate transport system. It is indicated that almost all large molecules and 98% of small molecules are not able to cross the BBB including drugs with molecular weight more than 400-500 dalton [8–10]. Due to the impermeability of BBB conventional drug administration commonly need continuous or repeated injection with high doses to reach the therapeutic dosage [8,10]. Therefore, drugs can directly administer to CNS via cerebrospinal fluids (CSF), novel drug delivery systems or by manipulating BBB [4].

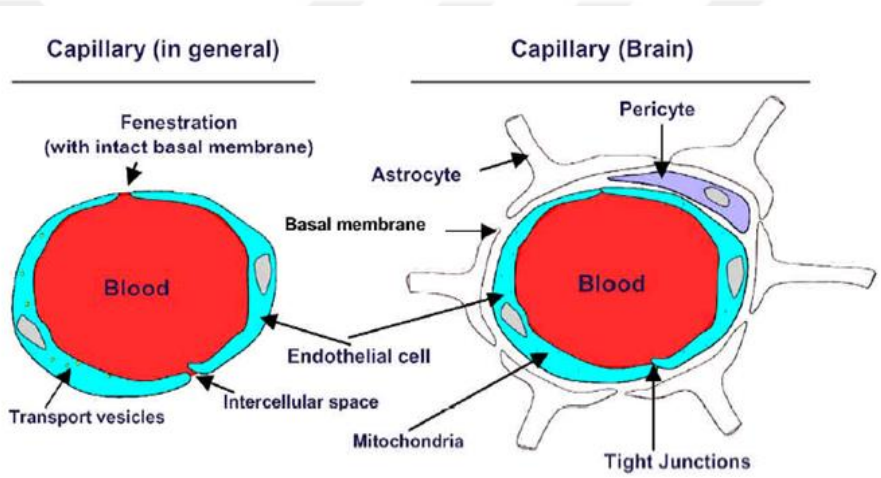

Figure 1.1: Comparison of capillaries in general and brain [11]

Biomaterials including hydrogels, particles and fibers are attractive for local drug delivery with therapeutic agents to treat CNS disorders. These forms of biomaterials are advantageous to provide multifunctional design options, tuning of mechanical properties promotion of cell proliferation and tissue regeneration. Most importantly, materials and their residuals should be biocompatible and not cause any adverse effects. Drug release should be adjustable to achieve demanded profit. Biomaterials may extend drugs' half-life and provide sustained release instead of burst release. Drug release can be adjusted by both degradations of biomaterial and diffusion of the therapeutic agent [10,12].

N, N0-bis[2-chloroethyl]-N-nitrosourea (BCNU; carmustine) has been used as a therapeutic agent for the treatment of glioma. Although carmustine can cross BBB, clinical use of carmustine is limited due to high systemic toxicity and short half-life which causes decreased bioavailability for tumors. To overcome challenges, carmustine is delivered to the lesion site in the form of a biodegradable wafer [13]. Brem et al. showed that carmustine delivery with wafer comprising poly[bis(p-carboxyphenoxy)propane]anhydride: sebacic acid and further radiation therapy was safe in primate brain [14]. In 1995, 222 patient with recurrent glioblastoma received randomly carmustine immersed wafer. The median survival of wafer implanted patients was 31 weeks while placebo patients' survival was 23 weeks. Also, 6-month mortality was found decreased to 44% with carmustine wafer from 64% among patients who have glioblastoma. Significant adverse effect was not observed associated with the wafer [15]. The commercially available form of wafer Gliadel® is an approved polymer mediated local delivery system as an adjunct to standard treatment of newly diagnosed high grade malignant glioma and recurrent glioblastoma multiforme (GBM). Biodegradable wafer composes of 1,3-bis-(p-carboxyphenoxy)propane and sebacic acid (20:80) at the molar ratio which contains 3.85% carmustine [16,17]. Studies showed that degradation of wafer was able to vary due to different chemical behaviours of polymers furthermore hydrophobic profile of copolymer prevented the rapid hydrolysis of carmustine. Therapeutic agent could be delivered at high doses within millimetres of implant area although more distant areas reached low concentration. This result was considered as favoured according to neurotoxicity. The release of carmustine was occurred through diffusion from wafer at first ten hours then while wafer was degrading, increased porosity of wafer eased the release [17]. 32 patients who had high grade gliomas (Grade III and IV) were studied to find out effectiveness of Gliadel wafers. Treatment was furthered by a standard radiotherapy for each patients and it is resulted that gliadel implanted patients had 18.2% longer median survival group than non-implanted group patient [18].

Nanofibers in the form of scaffold, matrix or substrate support cells mechanically. Besides that, nanofibers have a high surface area and porous structure also controllable surface properties which may be utilized for increased cell attachment or drug release etc. They can provide adjustable biodegradation and excellent biocompatibility according to used polymers[19,20].

Electrospinning a prominent technique for nanofiber fabrication in the interest of time and cost efficiency, ease of use and versatility (Figure 1.2). Electrostatic field between syringe and collector leads to the formation of Taylor cone and, a single fiber occurs when electrostatic forces overcome the surface tension of polymer drop which is followed by an immediate solvent evaporation and fiber deposition onto collector [21]. Distance between syringe tip and collector, concentration, conductivity, feeding rate and type of polymer solvents allow to tune diameter of nanofibers. Also, the electrospinning process can be affected by applied voltage amount, nozzle tip, flow rate, collector type, temperature or humidity [22,23].

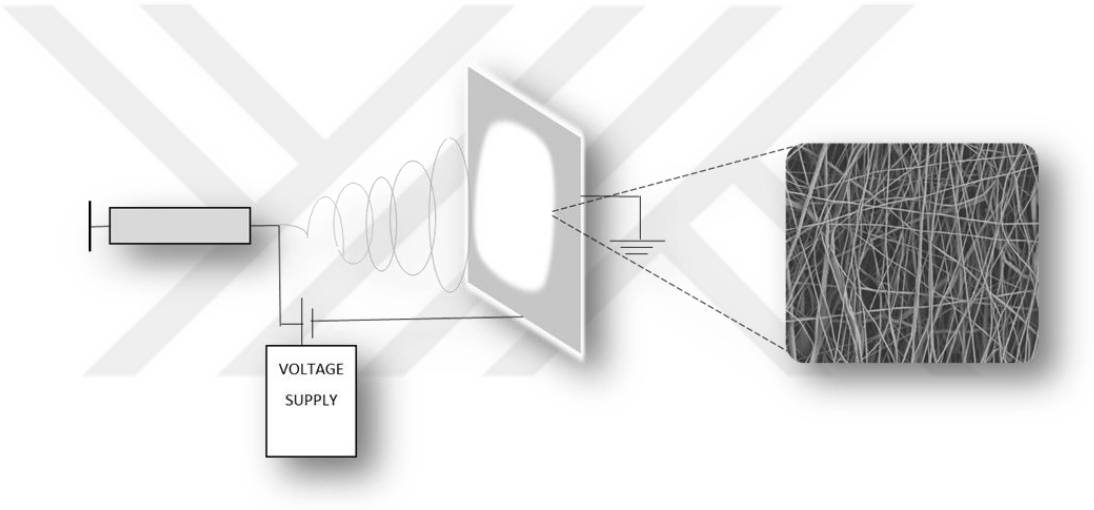

Figure 1.2: Basic electrospinning setup

Collagen, chitosan, cellulose, gelatin, polyvinyl alcohol (PVA), poly ε-caprolactone (PCL), poly (lactic-co-glycolic acid (PLGA) are some examples mostly used natural and synthetic polymers for electrospinning.

The high diversity for materials in electrospinning and Active Pharmaceuticals Ingredients (APIs) makes the electrospinning attractive for the development of drug delivery system by providing fibers with large surface area, ease of use, and controllable drug release by tuning degradation of fibers also, extensive drug loading capability. Specifically, challenges of delivering poorly water-soluble and bioavailable substances can be overcome with nanofibers[24]. Taking advantage of blend polymers

is getting attention to enhance the feasibility of electrospun fibers for also tuning the biocompatibility of fibers and drug release profiles from nanofibers. Kim. et al. prepared electrospun nanofibers by blending PCL and polyethyleneimine (PEI) at several concentrations and ratios. It was found that PCL/PEI electrospun nanofibers have a positive effect on cell viability compared to pristine PCL, however, increasing PEI ratio causes lower cell viability. Therefore, cell viability on PCL/PEI (20:1) at 20 wt. % concentration compared to pristine PCL by fluorescent staining and higher cell viability was observed on blend nanofiber. Moreover, the hydrophilicity of PCL was increased by blending with PEI to enhance cell adherence and proliferation with a proper porous structure. As a result of blending, PEI is a promising approach to overcome the limitations of PCL nanofibers and improve cell viability [25]. Although drugs can be loaded to nanofibers with several strategies as presented in figure 1.3, adequate drug amount and exposure time at the desired area are critical.

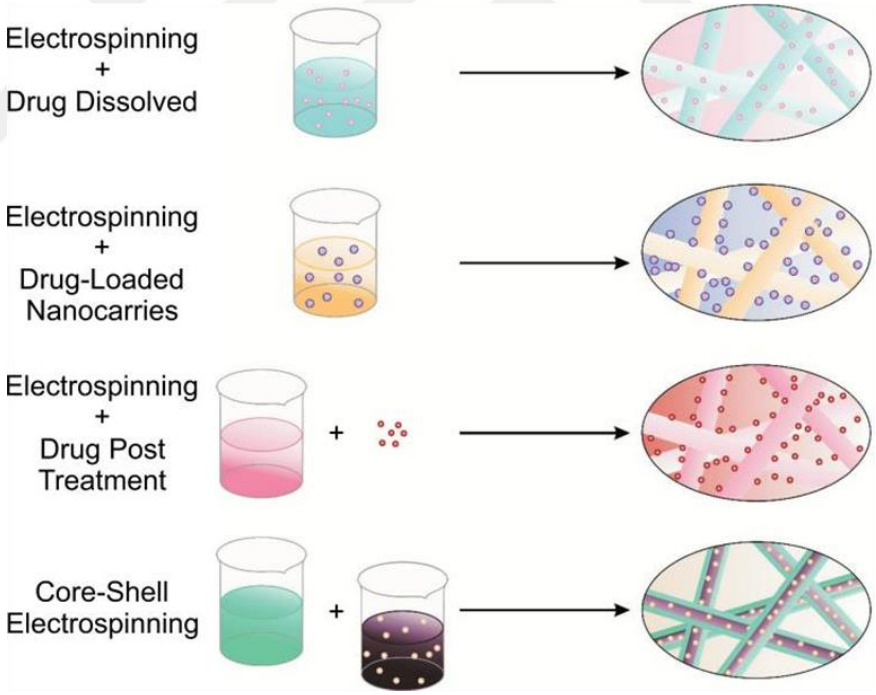

Figure 1.3: Several approaches for drug loading [24]

Biodegradable polymers such as PCL, PVA, and chitosan are widely used for drug loading to prevent post-surgery and high immune response [24]. Drugs can release by desorption from the surface, degradation of electrospun fibers and diffusion from

pores[26]. Composition and diameter of fibers, drug loading method, and surface modifications affect the release profile of drugs from nanofiber which is immediate, modified or delayed [20,23]. Directly entrapping drugs generally release immediately from biodegradable nanofibers and have a poorly controlled release profile [20]. Fibers composed of small diameter have faster release due to higher dissolution rate and surface area. Also, randomized nanofibers tend to water absorption more and exhibit faster release. However, low porous thin nanofibers have slower release than high porous thick nanofibers[26]. Conversely, sustained release can be achieved by using hydrophobic polymers or incorporation of drug loaded nanocarriers such as nanoparticles, liposomes into nanofiber matrix. An initial burst release followed by a sustained release is expected from nanofibers with these strategies [23]. This approach is useful when the highest drug dose is needed immediately followed by a sustained release to extend therapeutic effect or minimize further repeat. For instance, an immediate release might cause inhibition of tumor growth while sustained-release provides long-term therapy such as tumor recurrence[27].

Incorporation of poorly water-soluble drugs into nanoparticles aids for solubility improvement and protection of the drug molecule hence the bioavailability [28,29]. Most of the available nano-drug formulations are liposome-based formulations, such as Doxil [30]. However, the intrinsic instability and low drug-loading capacity of organic nano-drug formulations restrict their further clinical translations and leave them in the preclinical stage [31].

As a special architecture mesoporous silica nanoparticles (MSN) are emerging nanocarriers for therapeutic drug delivery to treat various problems including cancer, bone, and inflammation[32]. In recent years, MSN are notable materials due to their unique mesoporous structures and tunable pore size to control drug loading and release profile. Their large surface and pore volume allows for a high amount of drug loading and adsorption [33]. The fundamental characteristics of silicon dioxide (silica)-based nanoparticles, such as size, optical properties, high surface area, low density, adsorption capacity, capacity for encapsulation, biocompatibility, and low toxicity, make them an especially attractive inert solid in diverse biomedical applications [34].

Silanol groups on silica are commonly employed to be functionalized with a variety of chemical entities to control the interaction at biological interfaces [35]. For instance

amino, carboxyl, phenyl groups can be used for surface modifications. Surface functionalization is achieved through the outer particle surface and interior pore surface[36]. A sustained release can be achieved via surface modification which increases drug diffusion resistance due to the presence of functional groups or polymers [33]. Bare MSN with negative charge would interact with serum and clear rapidly into the bloodstream. Thus, surface modification is commonly needed to tune the surface reactivity, alter the cytotoxic effect and enhance biocompatibility, circulation time of MSN, efficiency, and loading of various kinds of drugs such as hydrophilic or hydrophobic [32,33,37].

Nanoparticles can be integrated with nanofibers via different strategies, such as blending [38,39],core-shell [40] or surface adhesion [41] to tune the drug release profiles Employing nanoparticles with nanofibers alters the release kinetics and allows the dual or multiple drug molecule loading. Therefore, Xie et al. designed a scaffold for promoting cell proliferation and angiogenesis at different phases of healing with the relayed release of vascular endothelial growth factor (VEGF) and platelet-derived growth factor-BB (PDGF-BB). For this reason, VEGF was loaded into nanofibers by blending to receive a faster release while PDGF was encapsulated into PLGA nanoparticles which were embedded in nanofibers for sustained release. *In vitro* studies showed that designed nanofiber meshes were capable to enhance cell growth and accelerate the healing significantly *in vivo* [42]. Integration of drug-loaded nanoparticles to nanofibers is also emerging for cancer treatments to take advantage of local delivery and controllable release profile. As an example, doxorubicin containing silica nanoparticles were blended into chitosan/PLGA to fabricate nanofibrous mats. Results have shown that these nanofibrous mats provide sustained release of doxorubicin and inhibition of HeLa cells growth. Thus, it was expected nanofibrous mats might display long-term antitumor efficiency. Also, the damage was observed with transmission electron microscopy on silica nanoparticles to affirm the degradation of silica nanoparticles. Therefore, mats are great candidates as implantable drug delivery systems especially for cancer reoccurrence [43]. Spin coating is one of the fastest and affordable techniques to integrate nanoparticles and nanofibers [44]. To enhance solubility and bioavailability especially for hydrophobic drugs, a solid dispersion approach can be received by spin coating technique in the crystalline or amorphous state [45]. Spin speed, surface wettability, and colloidal

concentration are critical parameters to control film formation [46]. Also, samples might need to treat before spin coating to alter their surface wettability such as by immersing into a solution for hydroxylation [46].

In this study, it is aimed to develop a nanoparticle-integrated nanofiber based local drug delivery system and to evaluate its performances to be employed as a synthetic dura graft. Dura is a membrane that encloses nerve tissues in the brain and spine to provide a barrier against CSF leakage and mechanical damage. However, most brain and spine surgeries cause discontinuity of the dura membrane therefore, autograft, allograft, xenograft or synthetic grafts are used to provide integrity [47–50]. It is crucial that grafts should not cause immunologic response or inflammation while supporting wound healing and preventing CSF leakage at the lesion site [51]. Although autografts have minimum immunologic response their use is limited because of local morbidity and fewer convenient tissue [52]. On the other hand, Creutzfeldt–Jakob disease was associated with allografts made of cadaver [53]. In the case of xenografts, inflammation and prone to reabsorption are challenging [54]. Eventually, synthetic materials are getting attention to design novel dura grafts. In addition, MacEwan et. al showed that a nanofabricated synthetic dura substitute executed less inflammation, irritation and fibrosis than xenograft material as well as providing a convenient closure at the lesion site as well as [54]. Electrospun nanofibers are noticeable for dura substitutes considering their adjustable diameter or mechanical properties and interconnected porous structure, but they do not encounter behaviors similarly living tissue [55]. Although the incorporation of therapeutic agents with nanofibers is noteworthy to improve functionality drug release profile is associated with direct fiber degradation which hinders the use of hydrophobic polymers such as PCL [24,56].

In view of the aforementioned information, a novel local drug delivery system was designed on the subject of dura substitute for wound healing and tissue regeneration. Correspondingly, curcumin was used as a model for poorly soluble drugs additionally its antitumor, anti-inflammation, wound healing, or antioxidant properties [57–60]. Curcumin was carried into MSN to enhance its bioavailability and solubility moreover curcumin-loaded MSN integrated with PCL and PCL-PEG: PEI nanofibers by spin coating technique. Nanofibers were fabricated by blending PCL and PEG: PEI

copolymer at varied ratios (100-1,200-1,250-1,300-1 w/w) to take advantage of mechanical resistance and biocompatibility of PCL additionally hydrophilicity of mPEG: PEI copolymer to increase cell attachment and migration that can take role in dura regeneration. Nanofibers were characterized concerning morphology, water absorption, biodegradation, cytotoxicity, and surface wettability. MSN were grafted with polypropylene imine (PPI) to enrich the amine functional group and loaded with curcumin (MSN-Cur). MSN were evaluated in terms of morphology, hydrodynamic radius, polydispersity index, surface charge, loading capacity, cytotoxicity, pore size and amine functionalization. As a result of the characterizations above, nanofiber and nanoparticle experimental groups were minimized. Furthermore, curcumin-loaded MSN were accommodated onto electrospun nanofibers which enables to diversify drug release profile and adjustable dosage. But, cold atmospheric plasma (CAP) was applied onto nanofibers before accommodation for increasing surface wettability to achieve homogeneous thin layer coating with MSN-Cur. Similarly, morphology, cytotoxicity, release profile, content and migration test were performed on nanoparticle accommodated nanofibers.

To the best of our knowledge, a design of MSN integrated electrospun nanofiber for poorly water-soluble drugs does not present as a dural substitute in literature. The designed drug delivery system is considered novel in dura studies due to its tunable release profile apart from polymer degradation. Another key thing to remember the use of cold atmospheric plasma and spin coating approaches is noteworthy for drug delivery design. We strongly believe that our novel local drug delivery system contributes to the literature greatly with tunable dosage and release profiles for poorly soluble drugs as well as assisting tissue regeneration.

Chapter 2

2.1. Materials and Methods

2.1.1. General

The thesis work encompasses there steps of designing a local drug delivery system for dura regeneration as shown in the flow chart below (Figure 2.1). In the first part of the thesis nanofibers, the different compositions of polymer blends were prepared to obtain electrospun fibers. The obtained electrospun nanofibers (NF) were characterized to investigate their morphological features, wettability, and water absorption rate, biodegradation and the cytocompatibility investigations and the polymer blend providing the most biocompatible and the most appropriate water absorption rate[61] to support dura regeneration employed to prepare nanofibers based local drug delivery system. Mesoporous silica nanoparticles (MSN) were prepared as the hydrophobic drug carriers and to be spin-coated on the nanofiber composition. The final composition of MSN with curcumin loading (MSN-Cur) was characterized in the meant of curcumin carrier after obtaining the most dispersible MSN-Cur composition they were accommodated on nanofibers by spin-coating technique. The spin-coated MSN-Cur on NF were taken topological features, and the cytocompatibility investigations performed to predict the appropriateness for dura regeneration. In the second step of the thesis, MSN-Cur spin-coated NF were taken for observing the drug release profiles to evaluate the potential as a local drug delivery system. In the third step of the thesis work, fibroblast cell attachment investigations were performed to evaluate the *in vitro* performances of the designed local drug delivery system for dura regeneration.

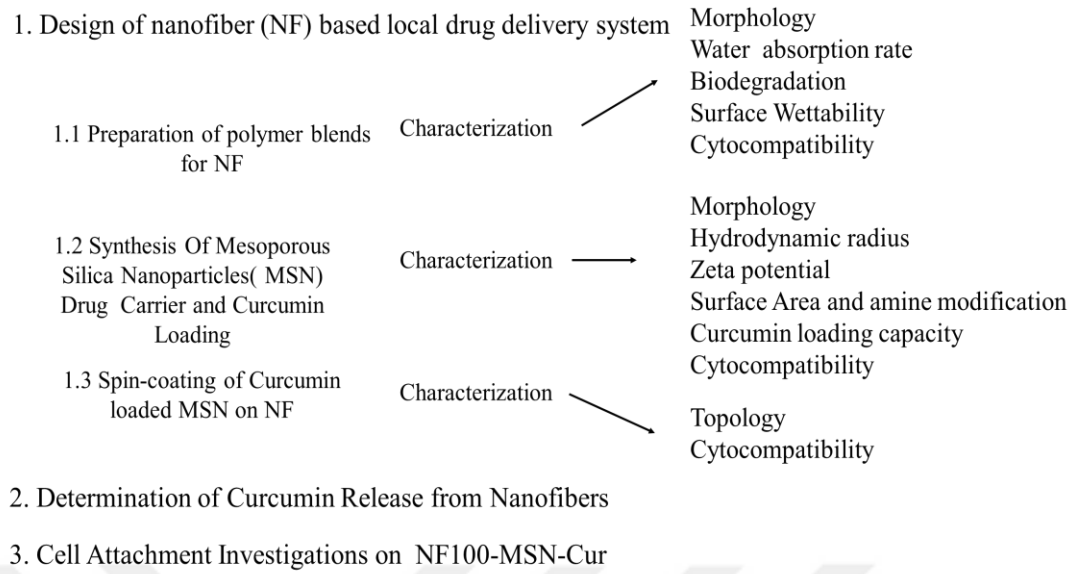

Figure 2.1: Scheme of methods

2.1.2. Design of NF Based Local Drug Delivery System

2.1.2.1. Preparation of Polymer Blends for Nanofibers

Before starting the electrospinning process poly(ethylene glycol) methyl ether: Polyethylenimine (mPEG: PEI)(50:1) copolymer synthesis was performed by following the literature protocols. Briefly, 3 g mPEG (5kDa; Sigma Aldrich) was dissolved in 10 mL chloroform under reflux at 60 ℃ following the addition of 9.5 mL hexamethylene diisocyanate (HMDI; Sigma Aldrich) to active -OH groups and stirred overnight. The next day, the polymer solution precipitated with diethyl ether and collected by 4500 rpm for 20 min. Activated PEG-aHMDI polymer was dried under vacuum. For PEI (25kDa; Sigma Aldrich) modification, 0.2 g of PEI dissolved in 10 mL chloroform and 2 g of mPEG was also dissolved in 50 mL chloroform. After that, PEI solution was added to mPEG dropwise at room temperature and let stir overnight under reflux at 60 ℃. Finally, the copolymer was precipitated with diethyl ether and centrifuged. The collected precipitate was dried under vacuum and stored at -20℃ for further use [62]. Copolymer refers to mPEG: PEI(50:1)(high) in the rest of the work. After obtaining the copolymer electrospun nanofibers were fabricated by blending PCL and mPEG: PEI(50:1)(high) in 5mL chloroform: dimethylformamide (3:1)

solvent at 10 %w/v ratio as well as PCL and mPEG: PEI(50:1)(high) ratios were arranged as 100-1,200-1,250-1 and 300-1 w/w and named as in Table 2.1 below. Electrospinning was conducted by using 20 kV electrical potential, 20 cm distance between needle and collector and 1mL/h pumping rate at room temperature. Fabricated nanofibers were stored in a vacuum desiccator.

Table 2.1: Fabricated electrospun nanofibers

Sample	Abbreviation
Pristine PCL	NF0
PCL-mPEG:PEI $(50:1)_{(high)}$ (100-1)	NF100
PCL-mPEG:PEI $(50:1)_{(high)}$ (200-1)	NF200
PCL-mPEG:PEI $(50:1)_{(high)}$(250-1)	NF250
PCL-mPEG:PEI $(50:1)_{(high)}$(300-1)	NF300

2.1.2.2 Characterization of Nanofibers

Morphology of Nanofibers

Fiber morphology was identified by scanning electron microscope (SEM; Carl Zeiss Microscopy, Germany). Humidity on nanofibers was removed by vacuum before observation. Nanofibers were cut as 0.5 x 0.5 cm square shape and coated with gold before the examination (QUORUM; Q150 RES; East Sussex; United Kingdom). The diameter histogram of nanofibers was found by MATLAB ver. R2017a).

Water Absorption Rate of Nanofibers

To perform a water absorption test, all nanofibers were cut as 1x1 cm squares from the area of each nanofiber that has a similar thickness. Each sample was dried well and humidity was removed. Shortly, each sample was weighed before the test and recorded as W1. Then, each nanofiber was soaked into a phosphate buffer solution (pH≈7,2; 10 mM,) and gently shaken for 24h at 37 °C and 150 rpm. The next day, soaked samples were weighted and recorded as W2. Water absorption was performed

in 3 replicates and each nanofibers' weights were measured 3 times and statistically analyzed using ordinary one-way ANOVA Tukey's multiple comparisons test by GraphPad Prism version of 8.4.2. The absorbed water amount relative to the initial weight of nanofibers were found by employing the equation 2.1 below[61];

$$\%W = \frac{W2\text{-}W1}{W1} x100 \quad (2.1)$$

Biodegradation of Nanofibers

First, artificial cerebrospinal fluid (CSF) contains 124mM NaCl, 2 mM KCl, 2mM $MgSO_4$, 1.25 mM NaH_2PO_4, 2mM $CaCl_2$, 26mM $NaHCO_3$, 10 mM D-glucose were prepared in sterile water (pH≈7.4)[63]. Then, nanofibers were cut as 1x1 cm and dried by vacuum-oven overnight. After weighting (W1), nanofibers were soaked into artificial CSF at 37 °C and shake gently at 150 rpm. Nanofibers were weighted as W2 at 1st, 2nd,7th,14th and 28th days. Before weighting, nanofibers were washed with distilled water roughly twice to prevent mineralization and dried for 48h again in a vacuum oven to remove CSF thoroughly. The experiment was performed in triplicate and each nanofiber was weighted three times. Results were statistical analyzed with two way ANOVA- Tukey's multiple comparisons test by GraphPad Prism version of 8.4.2. The deficiency of nanofibers' weight was calculated according to equation 2.2 given in below ;

$$\%D = \frac{W1\text{-}W2}{W1} x100 \quad (2.2)$$

Determination of Surface Wettability

Contact angle test was performed to assess hydrophilicity of NF0, NF100 and NF250 surface according to cytotoxicity and water absorption results. First, nanofibers were cut into 1x1 cm and attached cover glass to have straight surfaces. The attached nanofibers dried under vacuum before analysis. Contact angle (θ) between water drop and sample surface measured by Attension Theta.

Cytotoxicity of Nanofibers

Cytotoxicity of nanofibers given in Table 2.1 was tested by extraction method according to ISO 10993-5. Nanofibers were dried in an oven for 3days and cut in rectangular (2 x 3cm) shape then each surface was sterilized by ultraviolet radiation for 1h. Then, they immersed in 1 mL complete medium for (24±2)h at (37±1)℃ to extract their reservoir. After that, L929 fibroblast cells at the concentration $7x10^3$ cells/well were exposed to extractions and cell viability was determined for 3 days by 3-(4,5-Dimethylthiazol-2-yl)-2,5-diphenyltetrazolium bromide (MTT) assay. Cells were incubated with 10µl MTT stock solution (5mg/mL) and 100µl serum-free medium. Formazan crystals dissolved with dimethyl sulfoxide (DMSO) and absorbance of viable cells was measured by multi-mode spectrophotometry at 570 nm. Results were analyzed statistically with two-way ANOVA, Tukey's multiple comparisons test by GraphPad Prism version of 8.4.2.

2.1.2.3 Synthesis of Mesoporous Silica Nanoparticles Drug Carrier and Curcumin Loading

MSN were synthesized by the sol-gel method. Cetyltrimethylammonium bromide (CTAB) was used as a structure-directing agent and tetraethyl orthosilicate (TEOS) was used as a silica source. Briefly; the synthesis solution was prepared by mixing the reagent at the molar ratios in the given order 936.144 H_2O: 0.121 CTAB : 0.308 NaOH: 72.8 EtOH: 1 TEOS. Fluorescein-5isothiocyanate (FITC) labeling was prepared by mixing FITC and aminopropyl triethoxysilane (APTES) at the molar ratios of 1:3 in 2mL ethanol for 2 hours under vacuum. FITC solution was added to the synthesis solution after adding EtOH and finally, TEOS was added dropwise. The ratio between TEOS and APTES was calculated as 100:1. The synthesis solution was let stir overnight at 33 ℃ and protected from direct light. Structure directing agent (CTAB) was removed by employing solvent extraction 3 times and afterward washed with absolute ethanol as the final step of extraction and dried for further usage[64] and referred to as MSN-F.

Amine functionalization of MSN was performed by surface modification with polypropylene imine (PPI) to improve the drug loading capacity. Firstly, MSN were

dried under vacuum for 20 min and transferred to a Schlenk tube. 50 mg MSN were well sonicated in 5 mL toluene. After that, 5 µl acetic acid and 50µl azetidine were added and the solution was vacuumed. The reaction was occurred with reflux and in oil bath at 60 ℃ for 24h. The next day, the solution was collected by centrifuge and washed three times with EtOH. FITC labeled and amine-functionalized MSN were marked as MSN-F-PPI and dried for further use [65–67].

Curcumin was loaded into MSN-F-PPI by solvent immersion method to obtain adsorption isotherm. Briefly, 20 mg MSN-F-PPI were dispersed in 10 mL cyclohexane and sonicated for 30 min. Curcumin with starting concentrations 5%,10%, 25%, 50% w/w were added to MSN-F-PPI suspensions and sonicated for 40 min then let stir 24h at room temperature. The next day, curcumin loaded MSN-F-PPI (MSN-Cur) centrifuged and dried in an oven [68,69].

2.1.2.4. Characterization of Mesoporous Silica Nanoparticles Drug Carriers

Morphology of MSN Before and After Surface Modification

MSN-F and MSN-F-PPI were dried under a vacuum oven for overnight to observe their morphology by SEM. In short, nanoparticle powders were transferred onto a sample holder and coated with gold before the examination. Average particle diameter was measured by Image J software before and after modification.

Hydrodynamic Radius and Zeta Potential of MSN

The polydispersity index (PDI) of MSN-F, MSN-F-PPI, and MSN-Cur were determined by dynamic light scattering (DLS; Malvern Nano ZS 90 Zetasizer).Surface net charge of MSN-F, MSN-F-PPI was determined by zeta potential measurements (Malvern Nano ZS 90 Zetasizer) and hydrodynamic radius by DLS. Samples were prepared in 4-(2-hydroxyethyl)-1-piperazineethanesulfonic acid buffer solution (HEPES; pH≈7.2) at a concentration of 200µg/mL by sonication to prevent further agglomeration.

Surface Area and Amine Surface Modification Characterization

Amine surface modification amount of MSN-F-PPI was confirmed by thermogravimetric analysis atmosphere (TGA; TA Instruments, The Q600) between 30-600 ℃ with 10℃/min under atmosphere and surface area of MSN-F were analyzed with Brunauer–Emmett–Teller (BET; Micromeritics Instruments, 3 Flex Physisorption) method.

Curcumin Loading Capacity of MSN

Curcumin loading capacity of MSN and adsorption isotherm were calculated by employing spectrophotometric measurements. Before starting the investigations standard curve of curcumin which was prepared by dissolving curcumin in ethanol at 1, 5,10,20,50,100,200 μg/mL concentrations were performed and the absorbance values were determined at a wavelength of 425 nm with UV-vis spectrophotometer (Perkin Elmer Lambda 950). During investigations 0.25 mg/mL MSN-Cur was dispersed in ethanol and the loaded curcumin from the MSN matrix was eluted in ethanol with the help of ultrahigh sonication and stirring for 2h. After that, the suspension centrifuged and supernatants measured spectrophotometrically at 425 nm and calculated by employing the standard curve equation.

Cytotoxicity of MSN as Curcumin Carrier

Cytotoxicity analyses of MSN-F-PPI were evaluated on L929 mouse fibroblast cells at concentration of $7x10^3$ cells/well in order to identify the safe dosing of MSN carrier to be employed with NF. Briefly, MSN-F-PPI were diluted at concentrations of 5,10,20,50,100,200μg/mL with cell culture medium and were added onto cells. Cell viability was quantified by an LDH Cytotoxicity WST assay (Enzo Life Sciences) according to manufacturer instructions. Results were analyzed statistically with two-way ANOVA, Dunnett's multiple comparisons test by GraphPad Prism version of 8.4.2.

2.1.2.5. Spin-coating of Curcumin loaded Mesoporous Silica Nanocarriers on Nanofibers

NF100 were selected for MSN-Cur accommodation as the NF100 composition with the highest cytocompatibility. First of all, nanofibers were cut circular and sealed on 12mm cover glass after those nanofibers were wetted with HEPES buffer solution containing 0.1% w/v tween80 to prevent structural damage and treated by air dielectric barrier discharge plasma that was operated at 20kHz, and 40kV with 2,64 mm of discharge gap for 2minutes to alter surface wettability.

Furthermore, MSN-Cur (40,100,200µg) was accommodated onto nanofibers by spin coater (Laurell Technologies Corporation; model WS-400BZ-6NPP/LITE) operating at 500 rpm for 5sec followed by 4000 rpm for 60sec (acl= 022 rpm). Spin coated nanofibers given in Table 2.2 below were dried at 30 ℃ overnight.

Table 2.2: MSN-Cur spin-coated nanofibers

Nanofiber	Initial amount of spin-coated MSN-Cur	Abbreviation
PCL-mPEG:$PEI_{(high)}$ (100-1)	40 µg	NF100-MSN-Cur(40)
PCL:mPEG:$PEI_{(high)}$ (100-1)	100 µg	NF100-MSN-Cur(100)
PCL-mPEG:$PEI_{(high)}$ (100-1)	200 µg	NF100-MSN-Cur(200)

2.1.2.6. Characterization of MSN Spin-coated Nanofibers

In this part of the study, the performances of NF with MSN-Cur accommodation was evaluated to investigate their potential as biocompatible local drug delivery system as synthetic dura grafts.

Determining the Topology of NF-MSN-Cur Drug Delivery System

Samples had given in Table 2.2 were investigated to determine nanoparticle distribution and morphology by SEM. Samples were dried at 30 ℃ in the oven for overnight to remove humidity and coated with gold before the examination.

Cytotoxicity of NF-MSN-Cur

Cytotoxicity of nanofibers from Table 2.2 was tested by direct contact method according to ISO 10993-5. Experimental groups had been shown in Table 2.2 were sterilized by ultraviolet radiation (UV) for 1h. In addition, NF100 and only cover glasses were performed as control groups. Before cytotoxicity investigations, L929 mouse fibroblast cells seeded onto 24 -well plate at the concentration $5x10^4$ cells/well. Cells were incubated overnight and let attach to plate surface. Next, cells were washed gently 2 times with sterile phosphate buffer saline to remove dead cells. After that, samples were placed carefully onto cells directly and incubated for 24h, 48h and 72h. Cell viability was determined with MTT assay for 3 days. Briefly, samples were removed and cells were washed gently 2 times with sterile phosphate buffer saline. Cells were incubated with 50µl MTT stock solution (5mg/mL) and 500 µl serum-free medium. Formazan crystals dissolved with DMSO and absorbance of viable cells was measured by multi-mode spectrophotometry at 570 nm. Results were analyzed statistically with two-way ANOVA, Tukey's multiple comparisons test by GraphPad Prism version of 8.4.2.

2.1.3. Determination of Curcumin Release from Nanofibers

Curcumin release was performed in phosphate buffer solution (pH≈7.2; 12mM) containing 0.1%w/v Tween80 which will be referred to as release medium in the rest of the work. NF100-MSN-Cur (100) and uncoated NF100 were immersed in a release medium in the shaker at 37 ℃ and 150 rpm. Curcumin release from samples was determined by measuring release medium at 0.5h, 2h, 4h, 6h, 8h, 24h, 30h, 48h, and 52h with spectrophotometry. Cumulative release amount was calculated with standard curve comprising various curcumin concentrations in release medium. Uncoated NF100 was used as background. The release profile was determined in 3 replicates

and measured 3 times. Results were analyzed statistically with Ordinary one-way ANOVA, Sidak's multiple comparisons test by GraphPad Prism version of 8.4.2.Also, spin coated curcumin amount was calculated on NF100. Briefly, spin coated NF100 were dissolved in chloroform at the concentration of 1mg/mL and curcumin absorbance measured with spectrophotometer at 420 nm. Curcumin amount were calculated by standard curve that comprising of varied curcumin amount and NF100 in chloroform.

2.1.4. Cell Attachment Investigations on NF100-MSN-Cur

The impact of NF100-MSN-Cur (100) on cell proliferation and attachment were investigated by L929 mouse fibroblast cell line. First of all, NF100-MSN-Cur (100) were sterilized for 1h under ultraviolet radiation and conditioned in a cell culture medium for 30 min. Each sample was seeded with 75µL L929 cell suspension ($3x10^4$ cells) and incubated for 2 hours for cell adhesion. After that, cell suspensions were removed, samples were washed with PBS once and a fresh cell culture medium was added to each sample. Cell nuclei stained by 4′,6-diamidino-2-phenylindole (DAPI) according to manufacture instructions (Merck Millipore, Catalog No.FAK100) to observe cell adhesion and proliferation on nanofibers at 2h, 24h, 48h and 7days.

Chapter 3

3.1. Results and Discussion

3.1.1. Design of NF based local drug delivery system

3.1.1.1. Characterization of electrospun nanofibers with different polymer blends

Morphology

The morphology of electrospun nanofibers was examined by SEM. It was observed that a random and porous structure (in Figure 3.1) was employed for all nanofiber groups as expected. Although blending of mPEG: PEI did not affect the random and porous structure of nanofibers, NF0 and NF250 exhibited slightly thick junction formation which might cause by inhomogeneity. Fiber diameter distribution was determined by MATLAB for each nanofiber group and found that NF0 average diameter was approximately 500 nanometer (nm) whereas blended nanofiber groups fabricated with diameter mostly less than 500 nm. Nanofiber diameters can be affected by polymer concentration, volatility, molecular weight, viscosity, polarity, surface tension, surface free energy or conductivity also electrospinning setup parameters such as nozzle and collector distance or humidity [70]. For instance, it has been shown that PEI blending into PCL solution was effective for tuning nanofiber diameter. It was found that PCL/PEI blended nanofibers had smaller average diameters (150.4±33 to 220.4±32 nm) than PCL (473.3±65.2 to 1475.9±91.1 nm) which provided a higher surface area to volume ratio for biological studies[25]. Similarly, our results revealed that mPEG: PEI blending did not alter the interconnected porous structure and morphology of nanofibers however, it causes the formation of nanofibers with a smaller diameter.

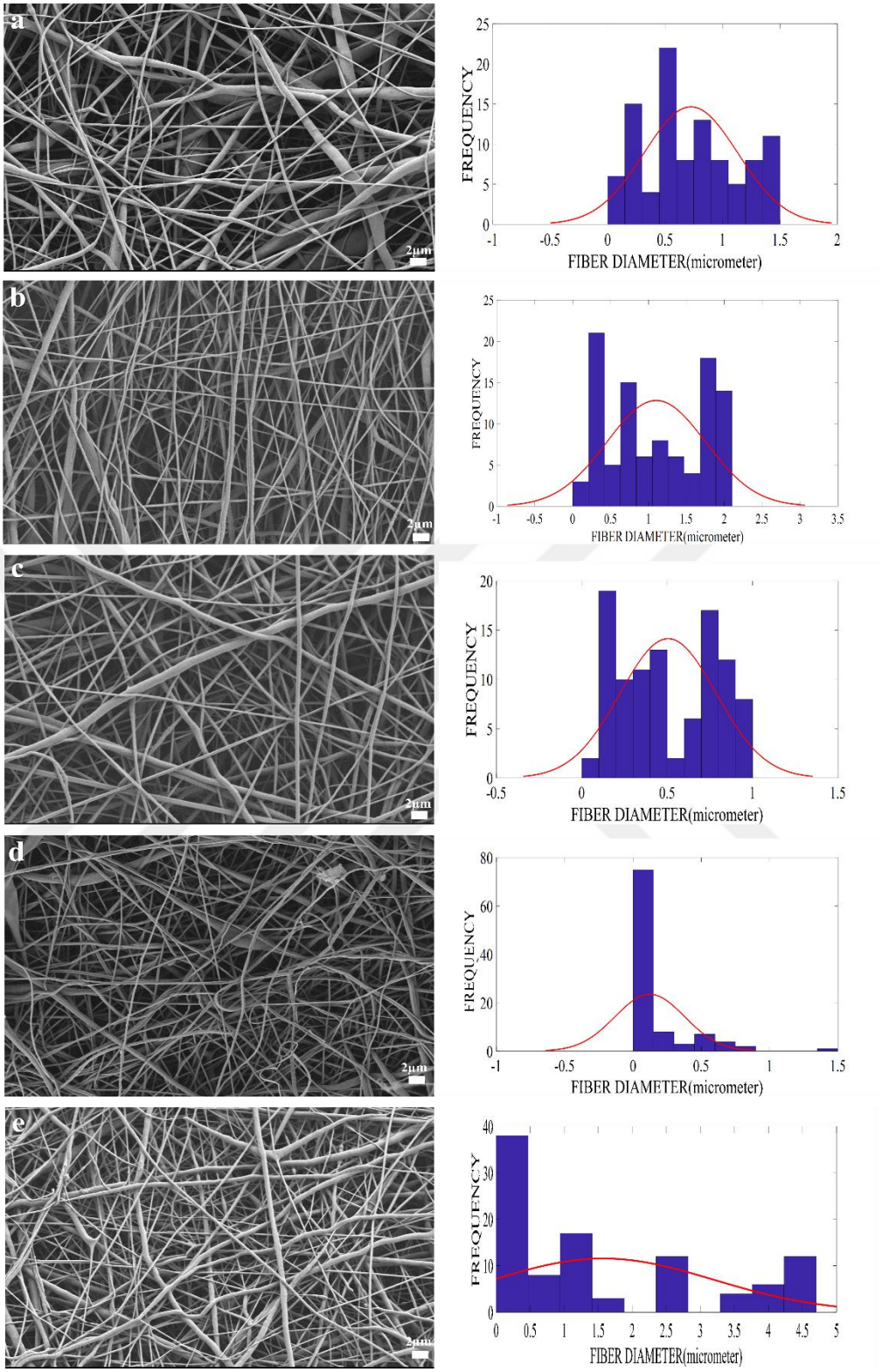

Figure 3.1: Electrospun nanofiber SEM images, (a) NF0, (b) NF100, (c) NF200, (d) NF250, (e) NF300

Water Absorption rate

Average thickness of nanofibers was measured approximately 50-100 micron by caliper. Water absorption of NF0, NF100, NF200, NF250 and, NF300 was found 57.72±35.05%, 42.42±10.4%, 4.9±3%, 41.7±26.4%, 10.5±4% respectively (Figure 3.2). Water absorption rate results did not show any significance according to the blending ratio of mPEG: PEI. The reason behind it was though for the varied water absorption rates might cause because of diversity in pore size and thickness of nanofiber groups. Wang et al. developed a nanofibrous dura membrane scaffold and compared it to commercial dura scaffolds. Their scaffolds showed 56.2 ± 2.1% water absorption rate whereas commercial scaffold's was 91.4 ± 2.3% and indicated that lower water absorption rate cause decreased stress on brain tissue [61]. In the light of literature, NF0, NF100 and NF250 which showed water absorption rate of nearly 50% were prominent groups for further experiments.

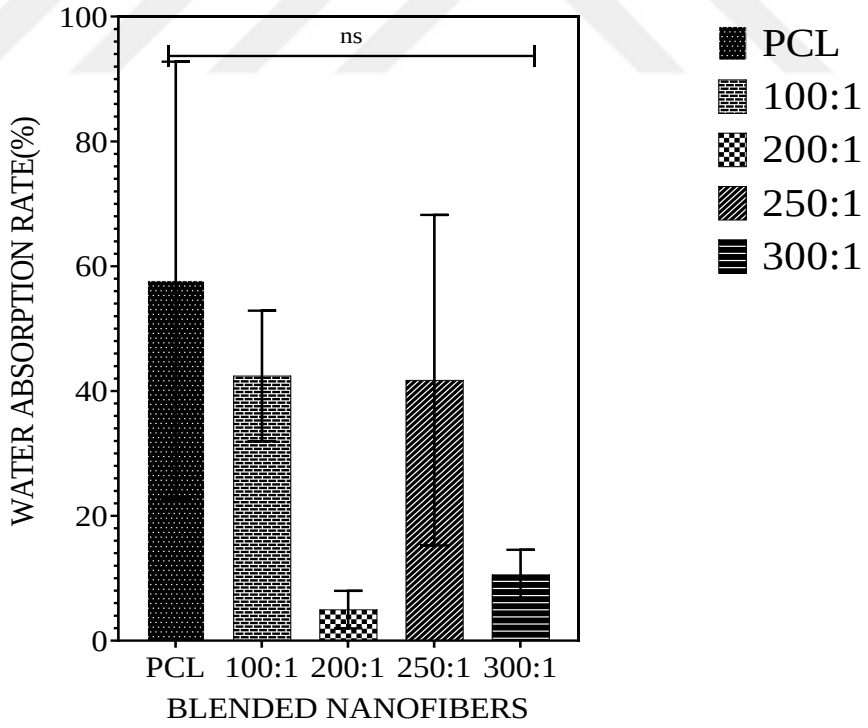

Figure 3.2: Water absorption rate of electrospun nanofibers. Data are represented as mean±SD. ns ($p \geq 0.05$) indicates no statistical significance.

Biodegradation and Wettability

Differently blending nanofiber did not show significant degradation except NF100 and NF200 during 14 days as it can be shown in Figure 3.3 because of the hydrophobic nature of PCL. PCL is known for its slow degradation rate which may last two to three years [71]. Similarly it has been shown in studies from literature nanofibrous scaffolds composed with PCL did not show degradation until 14 days and 8 weeks[72,73]. In addition, according to cytotoxicity results only NF0, NF100 and NF250 groups were investigated in terms of wettability. Several studies revealed that surface wettability can be enhanced by adding hydrophilic molecules into polymer solutions. Gordegir et al. indicated that blended PCL (Mw; 80.000) and PEI (50% w/v) nanofibers' surface contact angle was measured as 53.59° ± 3.17°, 49.7° ± 1.44° and 44.88° ± 4.04° respectively whether PCL-PEI ratios were 1:1, 1:2 and 2:1 w/w %[74]. Another study indicated that, methoxy polyethylene glycol (mPEG;Mw:5000) blended PCL (Mw: 70,000–90,000) nanofibers showed decreased contact angle in comparison to pristine PCL and as the mPEG ratio increased (PCL-mPEG (5, 10, 20, and 30%W/V)), surface contact angle(102±8°, 85±5°, 71±9°, 63±3° respectively) was found lower at the 1:1 PCL and mPEG ratio[75]. On the other hand, our contact angle analyses were showed that surface wettability of blend polymers did not alter according to pristine PCL (Table 3.1) and found in the range of 116–135◦ which is known for PCL[76]. Although there are studies in terms of adding mPEG and PEI that has decreased the surface contact angle our results were not corresponding. These results were concluded as the presence of mPEG content together with PEI (mPEG: PEI) in PCL blend promotes the amphiphilic nature and the PCL was predominant polymer into electrospun nanofibers[77]. Therefore mPEG: PEI did not alter the surface wettability and degradation because of the amphiphilic nature of blend. But, NF100 was treated with air dielectric plasma to overcome hydrophobicity. It was observed shortly after plasma treatment and wetting NF100 water contact angle was measured as 52.6 ° by Image J low bond axisymmetric shape analysis (LBADSA).

On the contrary insignificant degradation, certain nanofiber groups showed absorption. It was thought that the highly porous structure of nanofibers might induce absorption whereas the hydrophobic nature of PCL limits the degradation.

Table 3.1: Water contact angle of nanofibers

Nanofibers	Contact angle(°)
NF0	121.38±0.32
NF100	126.4±2.86
NF250	125.56±0.49

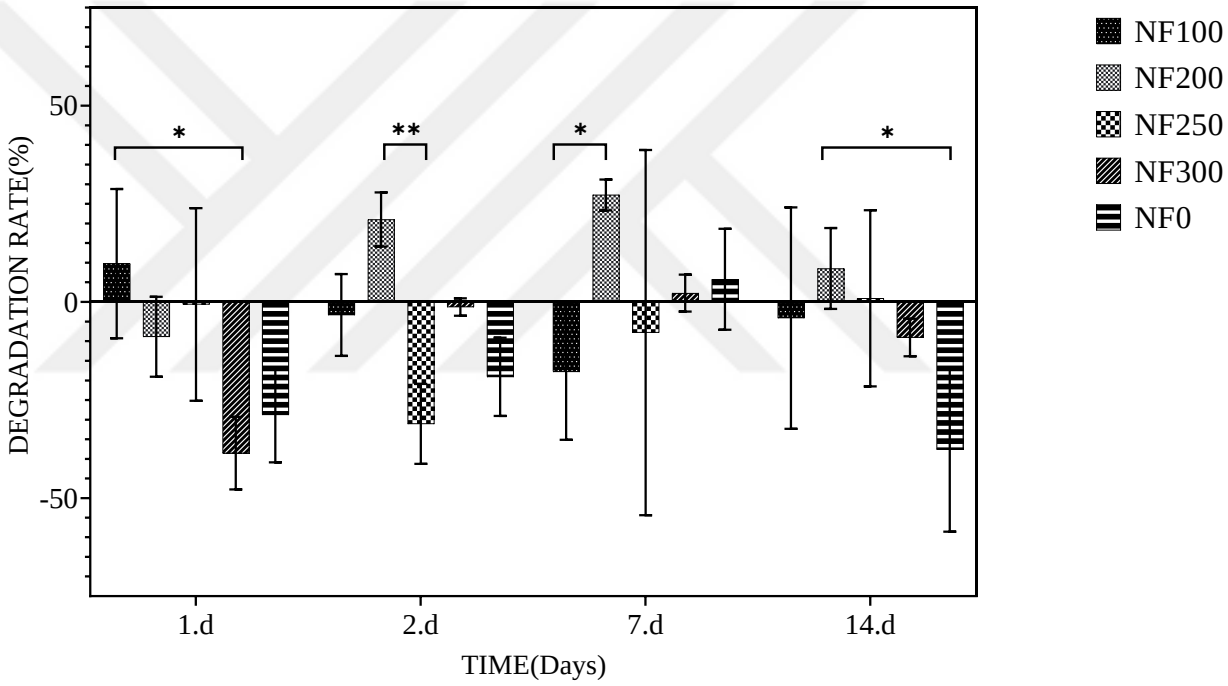

Figure 3.3: Biodegradation rate of electrospun nanofibers. Data are represented as mean±SD, **p < 0.01, *p < 0.05 no asterisk indicates no statistical significance.

Cytocompatibility

Cytotoxicity of nanofibers was performed with L929 mouse fibroblast cells by extraction method. It was showed in Figure 3.4 that all nanofibers show more than 60% cell viability at each time point. In detail, NF100 had the greatest cell viability

among all nanofiber groups for 24h. Although cell viability of NF100 reduced at 48h and 72 hours it was found nontoxic and had a similar or higher viability rate to its counterparts. Most importantly, NF100 has greater cell viability than pristine PCL for 72 hours where the lowest viability of NF100 was 85% as well. It was stated in literature PCL/PEI nanofibers allow more fibroblast viability as compared to pristine PCL due to the hydrophilic and cationic properties of PEI. In the contrast, an increased amount of PEI cause to decrease in viability [25]. Therefore, PEI can be modified to reduce toxicity with PEG biocompatible polymer. PEGylation of PEI is advantageous for increasing polymer solubility, biocompatibility and biodegradable linkages [78]. NF100 comprised of the highest mPEG: PEI as well as the lowest amount of PCL among nanofibers groups. Also, even there was no significance, NF100 was solely degraded for 24h approximately 10% relative to its initial weight. Therefore, it was considered the degradation of NF100 might cause mPEG:PEI release during extraction of it by immersing in cell culture medium for 24h. So, significantly increased cell proliferation of NF100 can be associated with degradation of nanofiber in 24h and positive effect of mPEG: PEI on fibroblast cells with less PCL content.

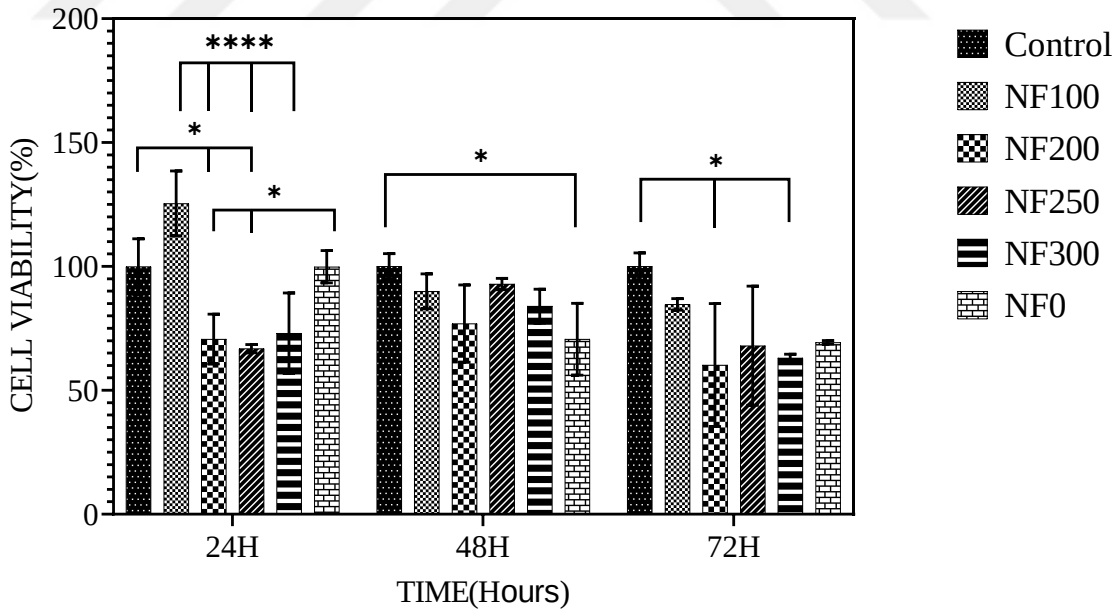

Figure 3.4: Cytotoxicity results of blended nanofibers at 24, 48 and 72 hours. Data are represented as mean±SD, ****$p < 0.0001$, *$p < 0.05$ and no asterisk indicates no statistical significance.

3.1.1.2. Synthesis of Mesoporous Silica Nanoparticles Drug Carrier and Curcumin Loading

Morphology

According to SEM images, spherical and non-aggregated nanoparticles were obtained. It was confirmed by SEM images in Figure 3.5 surface modification did not cause any morphological changes on MSN morphology. Average particle diameter was found 300 nm by measuring Image J software before and after surface modification.

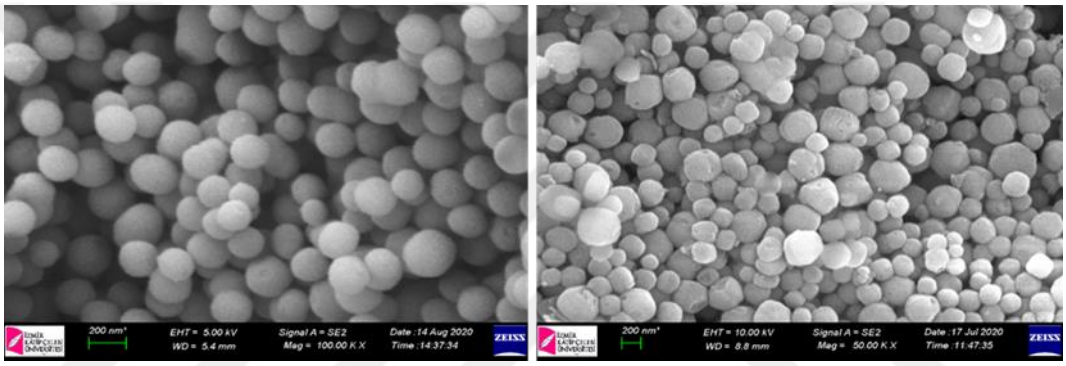

(a) (b)

Figure 3.5: SEM images of MSN before and after amine modification, (a) MSN-F, (b) MSN-F-PPI

Net Surface Charge and Hydrodynamic Radius of MSN

Zeta potential results shown in Table 3.2 pristine MSN-F had negatively charged due to silanol groups on surfaces however it was seen positively charge amine groups were grafted of MSN-F surface successfully. It was known that high magnitude of zeta potential aid to have well-dispersed nanoparticles. Amine modified nanoparticles did not show a significant difference in hydrodynamic diameter size. However, amine-modified nanoparticles had less hydrodynamic diameter which is indicated good colloidal stability. SEM diameter results and hydrodynamic radius of MSN were found consistent before and after surface modification. MSN in suspension showed larger diameter than powder MSN as it expected. Moreover, according to PDI values both

MSN were shown as monodisperse. But, it can be stated from Table 3.2 amine modification improved dispersibility of MSN-F due to obtained less than 0.1 PDI value which indicates perfectly uniform distribution [79].

Table 3.2**:** Zeta Potential and DLS results before and after surface modification

Nanoparticle Type	ζ Potential (mv)	Z-average (d.nm)	PDI
MSN-F	-16.3± 4.9	493.1±49.8	0.14±0.01
MSN-F-PPI	+25±5.3	328.2±9.3	0.03± 0.01

Surface Area and Amine Modification

The surface area of MSN-F was investigated by BET and found 1013 m^2/g. Result was revealed as high large surface area as typical MSN [80] which is advantageous for high drug incorporation and nanofiber integration. Amine modification amount on MSN-F-PPI was determined by TGA and the result showed that 7.8 w/w % of PPI was grafted successfully (Figure 3.6).

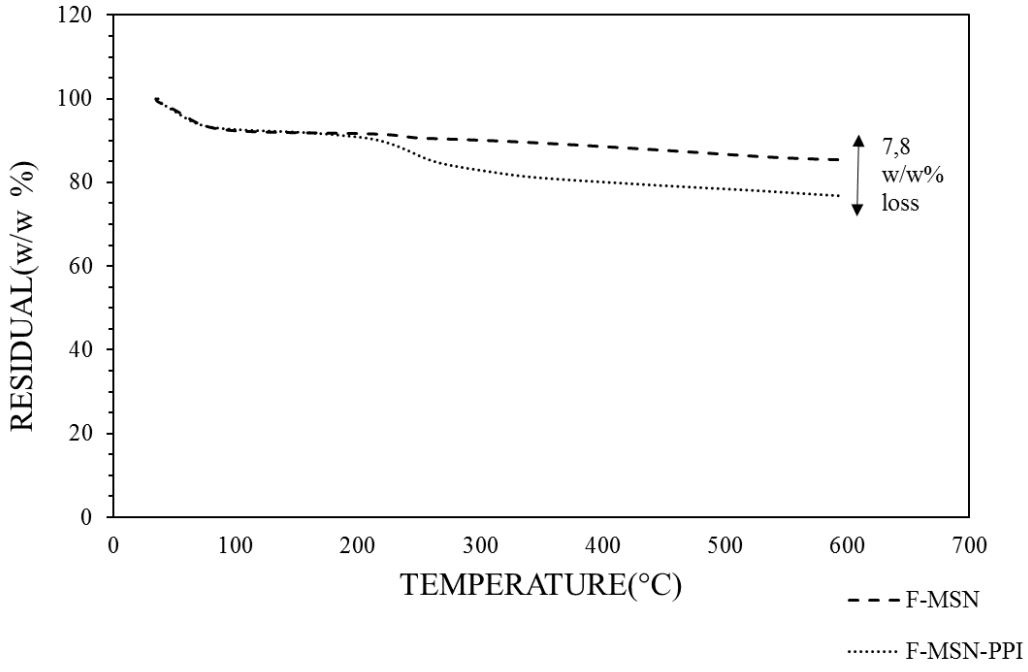

Figure 3.6: Amine modification amount

Curcumin loading capacity

Curcumin loading onto MSN-F-PPI showed linear adsorption isotherm. According to figure 3.7 initial concentrations 25% and 50% (w/w) had highest loading degree (w/w). To determine the concentration for further experiments both concentrations were loaded to MSN-F-PPI and their PDI values evaluated. Table 3.4 showed that PDI value of 25% w/w loaded MSN-F-PPI was found less than 50% loaded. Due to less PDI value employing a better dispersibility which is a significant for accumulation of nanoparticles on nanofiber curcumin loading was performed with 25%w/w starting concentration and the loading degree of curcumin into MSN-F-PPI was found 26.8w/w.

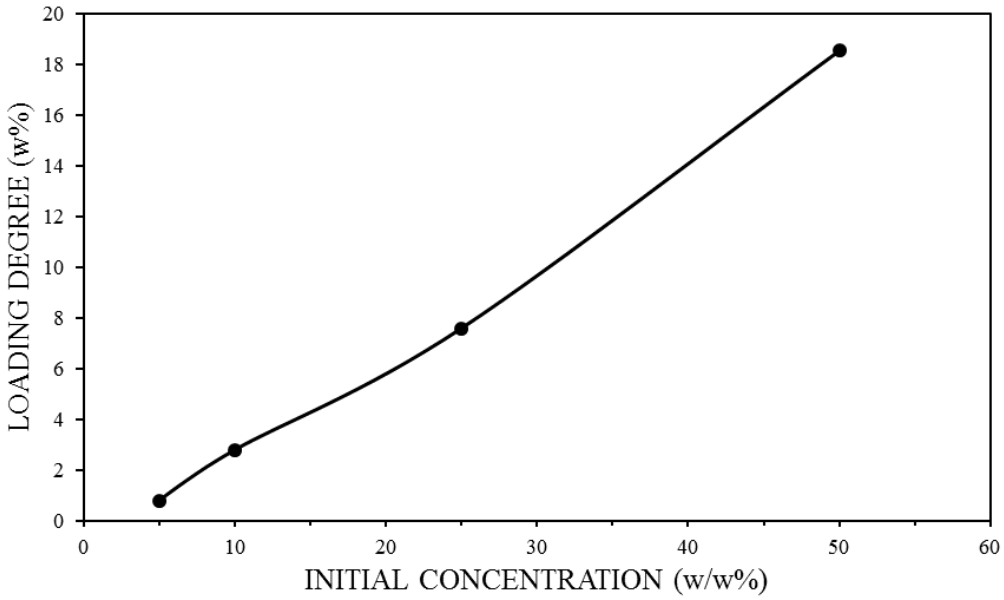

Figure 3.7: Curcumin loading adsorption isotherm

Table 3.3: PDI values of loaded MSN-F-PPI

Initial Concentration	PDI
25% (w/w)	0.244±0.044
50% (w/w)	0.264± 0.057

Cytocompatibility

L929 mouse fibroblast cells were treated with 5,10,20,50,100 and 200 µg/mL MSN-F-PPI suspensions for 48h. Results in figure 3.8 showed that cell viability has an insignificant decrease while nanoparticle concentrations increasing, however, only at 5 and 200 µg/mL concentrations were found significant for 24h in comparison to each concentration. More than 70% cell viability was measured for 5, 10, 20, 50, 100 µg/mL at 24h.The next day, MSN-F-PPI showed highly toxic effect at 20, 50, 100 and 200µg/mL concentrations although the cell viability did not decrease significantly at 5 and 10 µg/mL which referred that toxicity of MSN-F-PPI was concentration-dependent. Studies had shown that cationic dendrimers such as PPI were highly toxic both *in vitro* and *in vivo*[81] more than neutral or anionic dendrimers because of the tendency to bind negatively charged cell membrane [82]. Similarly, Najafi et al. showed that increasing grafting PPI dendrimer ratio onto gold nanoparticles cause to decrease in cell viability on human fibroblast cells due to cationic primary amines [83]. Although high toxicity, cationic groups are used in medical applications such as gene transfection [82]. Consequently, several strategies are needed to reduce the toxicity of cationic dendrimers while preserving their functionality.

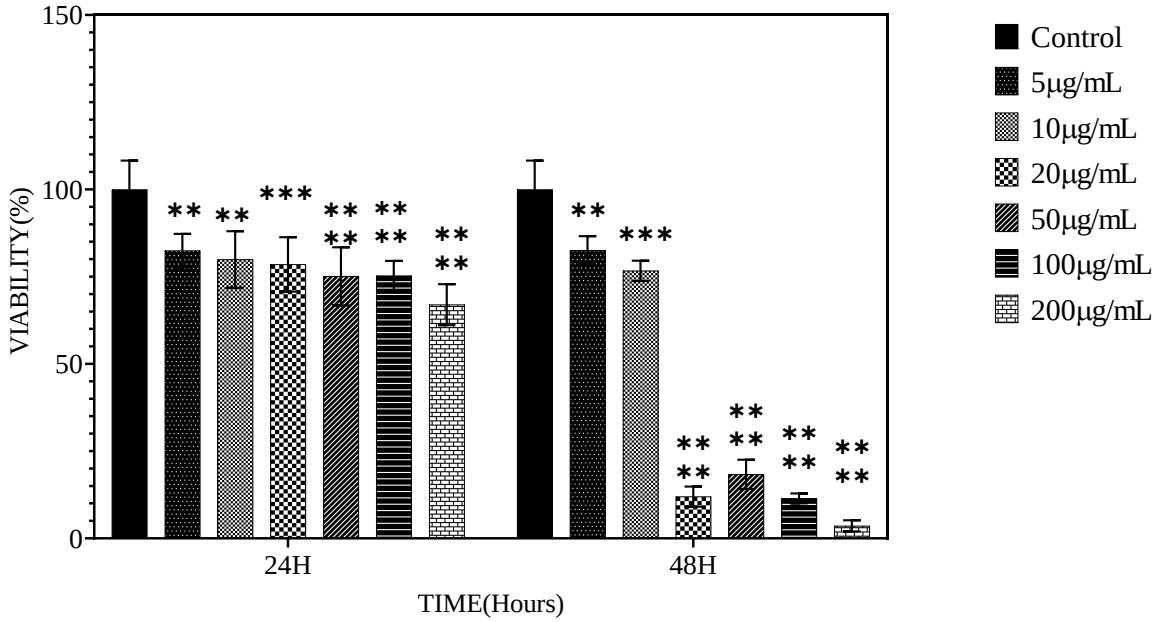

Figure 3.8: Cytotoxicity results of MSN-F-PPI. Data are represented as mean±SD, ****p < 0.0001, ***p <0.001,p** <0.01,*p < 0.05 and no asterisk indicates no statistical significance in comparison control group.

3.1.1.3. Spin-coating of Curcumin loaded Mesoporous Silica Nanocarriers on Nanofibers

Topology

Firstly, uncoated NF100 nanofibers were wetted with 0.1% tween 80 containing HEPES buffer and treated with air dielectric plasma to increase the surface hydrophilicity of PCL. It has been stated hydrophilicity of electrospun scaffolds can be improved by plasma treatment [84,85]. Air dielectric plasma parameters were optimized according to SEM of NF100 after treatment which did not cause morphological damage on nanofibers (Appendix A).

MSN-Cur were accumulated onto wetted nanofibers at various concentrations (40μg,100 μg and 200 μg) by spin coating technique at 4000 rpm with a spinning time of 1min. SEM images in Figure 3.9 showed that nanofibers kept their porous structure and did not damaged after spinning and air dielectric plasma treatment. Besides, nanoparticles preserved their spherical shapes onto surfaces and pores of nanofibers they clustered and not uniformly distributed. The heterogeneous distribution might occur due to local surface energy discrepancies and hydrophobic zones of nanofibers [46].

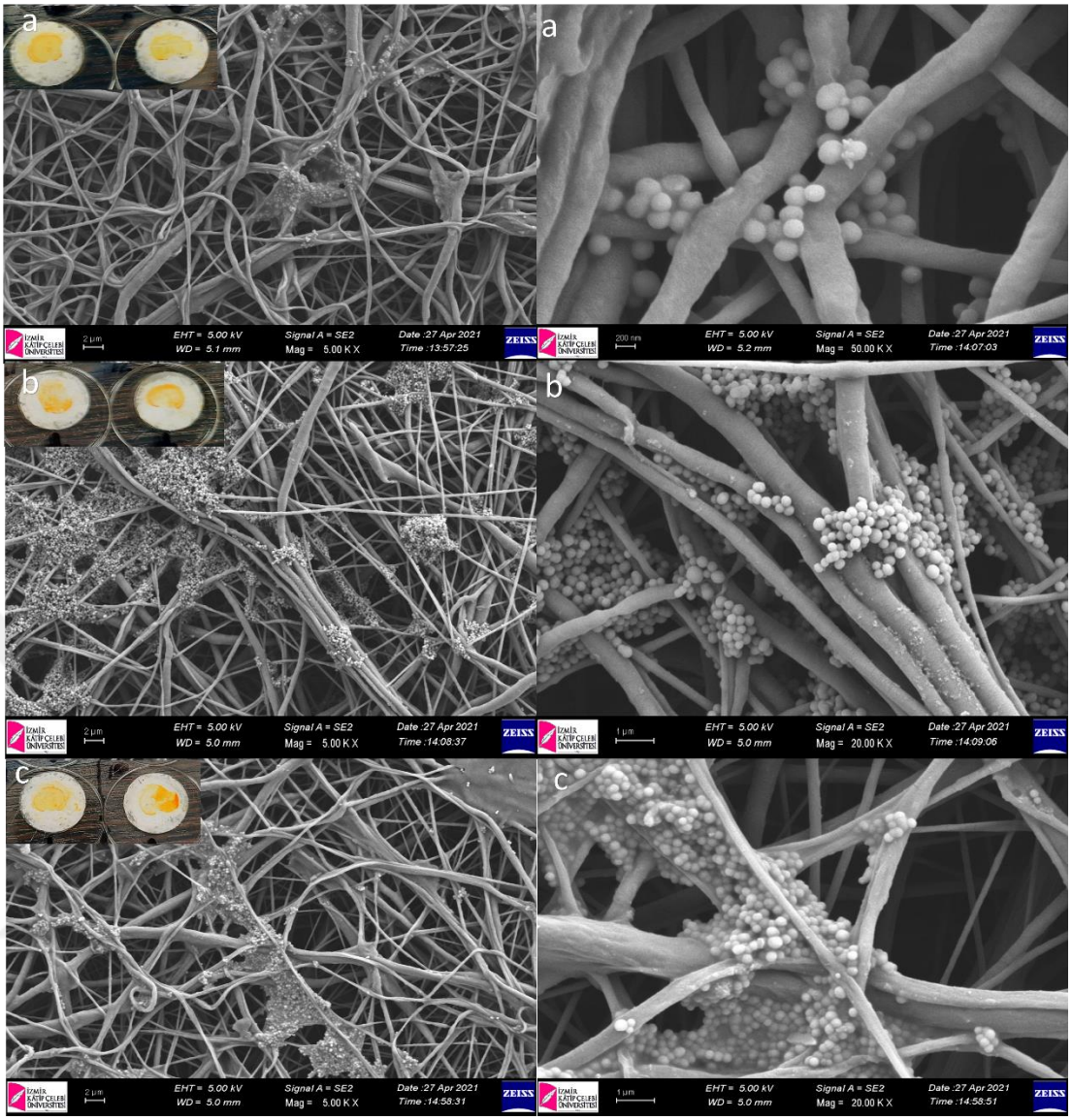

Figure 3.9: SEM images of spin coated MSN-Cur on nanofiber ,(a) NF100-MSN-Cur(40), (b) NF100-MSN-Cur(100), (c) NF100-MSN-Cur(200)

Cytocompatibility

Direct cytotoxicity of NF100-MSN-Cur (40), NF100-MSN-Cur(100), NF100-MSN-Cur(200), the test was performed on L929 mouse fibroblast cell line for 3days to determine the non-toxic concentration of MSN-Cur. Although in 2nd and 3rd days, starting concentration of MSN-Cur did not have any significance in figure 3.10, cell viability was found more than 80% for each group. Besides, MSN-Cur accumulated nanofiber induce cell viability for each concentration in 24h in comparison to the

control group. Most importantly, integration of MSN-F-PPI and NF-100 reduce the toxicity of MSN-F-PPI especially at high concentrations and enhance cell viability.

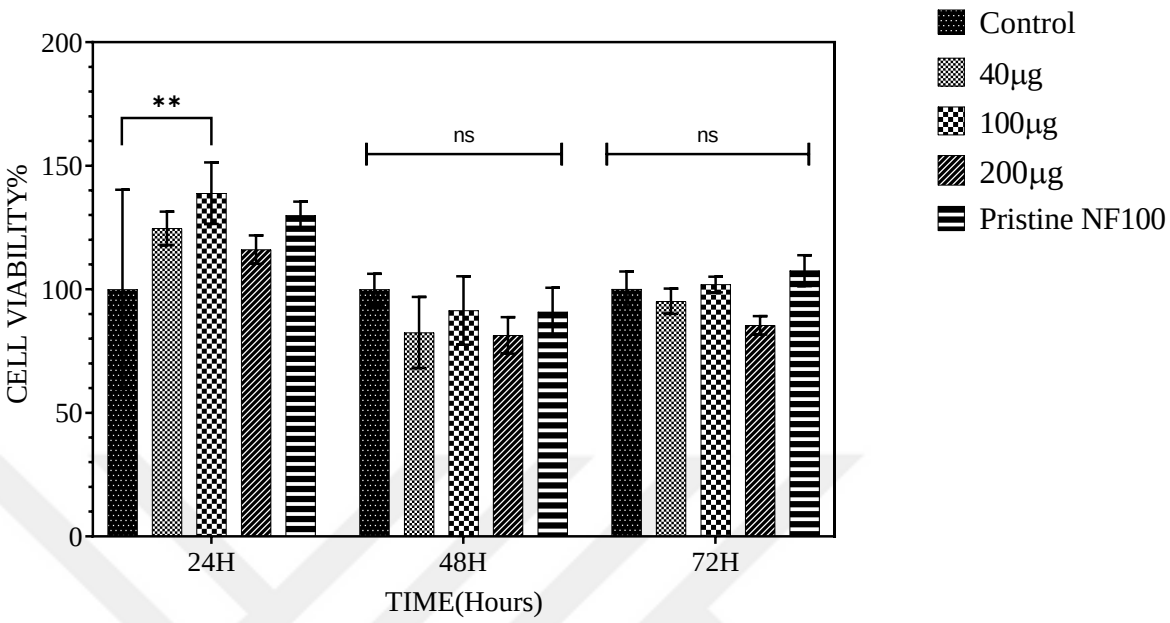

Figure 3.10: Cytotoxicity results of MSN-Cur spin-coated NF100, Data are represented as mean±SD, p** <0.01, and no asterisk indicates no statistical significance.

3.1.2. Determination of Curcumin Release from Nanofibers

Curcumin release profile was investigated in phosphate buffer solution containing 0.1% tween 80 for 0.5, 2, 4, 6, 8, 30, 48 and 52h (figure 3.11). Drug release from a biodegradable carrier is mainly occurred by polymer degradation or molecule diffusion thereby polymer properties are noteworthy to diversify drug release profile. For instance, diffusion of drugs is more expected instead of polymer degradation aided release in an aqueous medium for PCL due to its poor water solubility[86]. Spin coated curcumin amount was determined with standard curve in chloroform and it was found that 1 mg/mL NF100 accumulated with 0,160 µg/mL curcumin. It was observed that NF100-MSN-Cur (100) had a sustained release profile which allows the curcumin presence on the target area for a prolonged time. However, decreasing release amount was examined at 4h and 8h and it was thought that released curcumin into release medium was reabsorbed by nanofibers and caused decreased curcumin concentration

into surrounding release buffer according to the absorption capacity of nanofiber. In another view of results, our local drug delivery system showed curcumin release was independent of polymer degradation because of predominant polymer into the bulk structure of carrier was PCL which had little degradation in CSFs due to its high hydrophobicity. Curcumin was found into release medium during 52h with insignificant alterations that provides dose and frequency reduction and uniform drug amount at the targeted area over time. Also, the release profile of NF100 MSN-Cur (100) and cytotoxicity results were found consistent. It was concluded as cell viability can be affected by sustained release profile for long term. Results were indicated that our local drug delivery system successfully carried the hydrophobic drugs within MSN and corporation with nanofibers provided the sustained release.

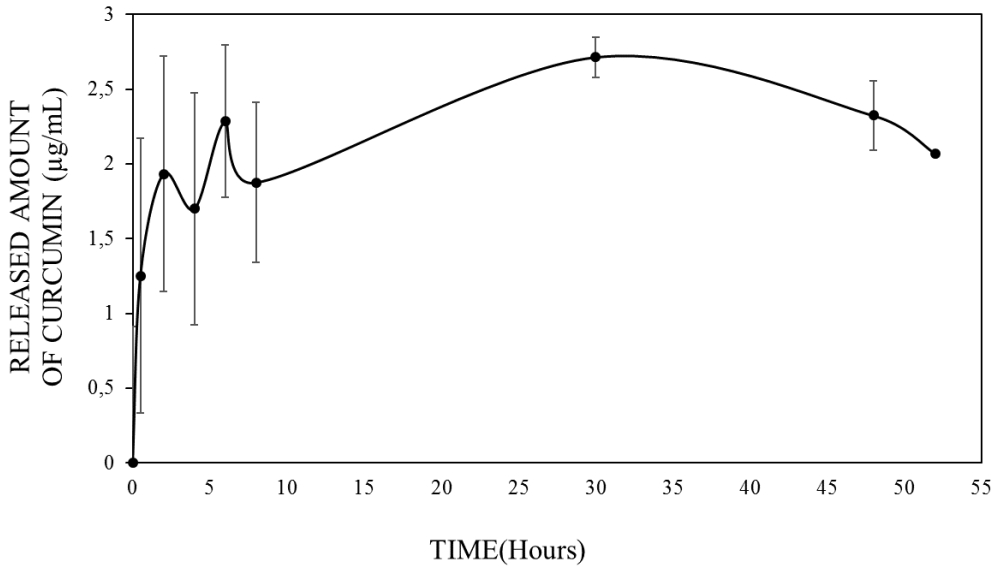

Figure 3.11: Curcumin release profile of NF100-MSN-Cur (100), Data are represented as mean±SD, no asterisk indicates no statistical significance.

3.1.3. Cell Attachment Investigations on NF100-MSN-Cur

Fibroblast cells adherence on NF100-MSN-Cur (100) were observed by staining cell nuclei with DAPI for 2h, 24h, 48h, and 7days (figure 3.12). Images showed that MSN-F-Cur (100) coating did not limit the fibroblast cells adherence to nanofibers. It was determined that MSN, curcumin, and nanofibers improve cell proliferation and cell

attachment. Existing silanol groups in silica cause an interaction with phospholipids which affects the cellular uptake. Moreover, silica nanoparticles are more stable against mechanical stress or degradation than liposomes and dendrimers because of the presence strong Si-O bond[36]. Quignard et al. examined the efficiency of soluble and nanoparticulated silica for migration and proliferation on human skin fibroblast cells. It was found that silica nanoparticles have a rapid effect and a delayed effect on wound healing due to the dissolution of particles thereby caused releasing of orthosilicic acid. However, positively charged silica nanoparticles enhance wound healing faster than soluble orthosilicic acid. Also, silica did not show toxicity in all forms tested and concentrations[87]. Our cell attachment results corresponded to drug release profile was effective on cell proliferation due to presence of at least 52 hours in the surrounding medium according to its sustained release profile. It was showed that drugs are effective on wound healing and cell proliferation processes overtimes by taking advantage of sustained release. Another advantage of our design was while MSN and incorporated drug employing therapeutic benefit for cells nanofibers provides a mechanical support and extracellular matrix like environment to enhance cell proliferation and tissue regeneration.

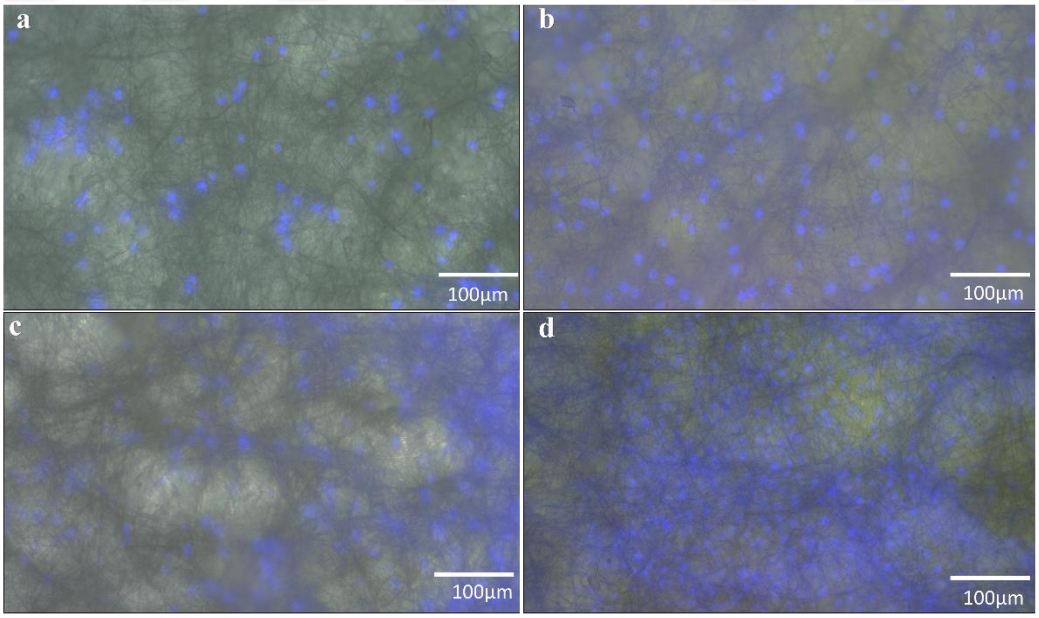

Figure 3.12: Microscope images of fibroblast cell adherence on nanofiber for (a) 2 hours, (b) 24 hours, (c) 48 hours, (d) 7 days (Magnification of images is 20x)

Chapter 4

4.1. Conclusion

Local drug delivery systems have a vital role to overcome limitations of conventional drug delivery approaches. Especially, delivery of hydrophobic drugs is needed to develop novel systems. Integration of nanofibers and nanoparticles can be served as a local drug delivery system to improve delivery of hydrophobic therapeutic agents whereas supporting the functionality of targeted site. In this thesis development of nanoparticle integrated nanofibers was evaluated as a dura substitute. Our results were revealed that nanofiber properties can be altered by varied blend composition and integration of nanofibers with nanoparticles limits the toxicity of nanoparticle suspensions. Cell attachment and cytotoxicity studies showed that, designed system did not have negative effect on cell viability contrary, it induced the cell proliferation at 24h. It was considered as sustained release enable to long term and controlled delivery of curcumin without polymer degradation and alter the cell viability. It was concluded that hydrophobic drugs can be successfully carried into MSN and released from nanofibers. It was achieved that our design enables to employ therapeutic activity directly at the lesion site while providing a mechanical support and a promotive environment for cell proliferation and tissue regeneration. Although interconnected porous and extracellular matrix like structure of nanofibers supplies mechanical reinforcement and cell attachment, detailed studies are needed for mechanical strength of nanofibers as a dura membrane substitute.

References

[1] Saka R, Sathe P, Khan W. Brain local delivery strategy. In: Gao H, Gao X, editors. Brain Targeted Drug Delivery System:A Focus on Nanotechnology and Nanoparticulates. Elsevier; 2019. p. 241–86. doi.org:10.1016/B978-0-12-814001-7.00011-1

[2] Shofner JP, Peppas NA. Overview of Biodrug Delivery Systems: Disease Fundamentals, Delivery Problems, and Strategic Approaches. In: Morishita M, Park K, editors. Biodrug delivery systems: fundamentals, applications and clinical development. New York: Informa Healthcare USA; 2010.

[3] Wen H, Jung H, Li X. Drug Delivery Approaches in Addressing Clinical Pharmacology-Related Issues: Opportunities and Challenges. AAPS J. 2015;17:1327–40. doi.org:10.1208/s12248-015-9814-9

[4] Jain KK. Current Status and Future Prospects of Drug Delivery Systems. In: Jain KK, editor. Drug Delivery System. New York, NY: Springer New York; 2014 p. 1–56. doi.org:10.1007/978-1-4939-0363-4_1

[5] Qureshi S, Khan W, Perez-Davidi M, Weiss EI, Beyth N, Domb AJ. Local Drug Delivery to the Oral Cavity. In: Domb AJ, Khan W, editors. Focal Controlled Drug Delivery. Boston, MA: Springer US; 2014. p. 285–304.doi.org: 10.1007/978-1-4614-9434-8_13

[6] Padrão T, Coelho CC, Costa P, Alegrete N, Monteiro FJ, Sousa SR. Combining local antibiotic delivery with heparinized nanohydroxyapatite/collagen bone substitute: A novel strategy for osteomyelitis treatment. Materials Science and Engineering: C. 2021;119:111329. doi.org: 10.1016/j.msec.2020.111329

[7] Federico C, Sun J, Muz B, Alhallak K, Cosper PF, Muhammad N, *et al*. Localized Delivery of Cisplatin to Cervical Cancer Improves Its Therapeutic Efficacy and

Minimizes Its Side Effect Profile. International Journal of Radiation Oncology*Biology*Physics. 2020; doi.org: 10.1016/j.ijrobp.2020.11.052

[8] Gabathuler R. Approaches to transport therapeutic drugs across the blood–brain barrier to treat brain diseases. Neurobiology of Disease. 2010;37:48–57. doi.org: 10.1016/j.nbd.2009.07.028

[9] Bors L, Erdő F. Overcoming the Blood–Brain Barrier. Challenges and Tricks for CNS Drug Delivery. Sci Pharm. 2019;87:6.

[10] Ziemba AM, Gilbert RJ. Biomaterials for Local, Controlled Drug Delivery to the Injured Spinal Cord. Front Pharmacol. 2017;8:245. doi.org: 10.3389/fphar.2017.00245

[11] Neerati P, Mohammad R, Bangaru R, Devde R, Kanwar. JR. The effects of verapamil, curcumin, and capsaicin pretreatments on the BBB uptake clearance of digoxin in rats. Journal of Pharmacy Research. 2012;5:2126–33.

[12] Chen J-C, Li L-M, Gao J-Q. Biomaterials for local drug delivery in central nervous system. International Journal of Pharmaceutics. 2019;560:92–100.

[13] Balossier A, Dörner L, Emery E, Heese O, Mehdorn HM, Menei P, *et al.* Incorporating BCNU Wafers into Malignant Glioma Treatment: European Case Studies. Clinical Drug Investigation. 2010;30:195–204. doi.org: 10.2165/11532900-000000000-00000

[14] Brem H, Tamargo RJ, Olivi A, Pinn M, Weingart JD, Wharam M, *et al.* Biodegradable polymers for controlled delivery of chemotherapy with and without radiation therapy in the monkey brain. Journal of Neurosurgery. 1994;80:283–90.doi.org: 10.3171/jns.1994.80.2.0283

[15] Brem H, Piantadosi S, Burger PC, Walker M, Selker R, Vick NA, *et al.* Placebo-controlled trial of safety and efficacy of intraoperative controlled delivery by biodegradable polymers of chemotherapy for recurrent gliomas. The Lancet. 1995;345:1008–12. doi.org: 10.1016/S0140-6736(95)90755-6

[16] Lillehei KO, Kalkanis SN, Liau LM, Mydland DE, Olson J, Paleologos NA, *et al*. Rationale and design of the 500-patient, 3-year, and prospective Vigilant ObservatIon of GlIadeL WAfer ImplaNT registry. CNS Oncology. 2018;7:CNS08. doi.org: 10.2217/cns-2017-0036

[17] Fleming AB, Saltzman WM. Pharmacokinetics of the Carmustine Implant: Clinical Pharmacokinetics. 2002;41:403–19. doi.org:10.2165/00003088-200241060-00002

[18] Valtonen S, Timonen U la, Toivanen P, Kalimo H, Kivipelto L, Heiskanen O, *et al.* Interstitial Chemotherapy with Carmustine-loaded Polymers for High-grade Gliomas: A Randomized Double-blind Study. Neurosurgery. 1997;41:44–9. doi.org: 10.1097/00006123-199707000-00011

[19] Sun Y, Cheng S, Lu W, Wang Y, Zhang P, Yao Q. Electrospun fibers and their application in drug controlled release, biological dressings, tissue repair, and enzyme immobilization. RSC Adv. 2019;9:25712–29. doi.org: 10.1039/C9RA05012D

[20] Cui W, Chang J, Dalton PD. Electrospun Fibers for Drug Delivery. Comprehensive Biomaterials. Elsevier; 2011. p. 445–62. doi.org: 10.1088/1468-6996/11/1/014108

[21] Mehetre G, Pande V, Kendre P. An Overview of Nanofibers as a Platform for Drug Delivery. Inventi Rapid: NDDS. 2015.

[22] Baji A, Mai Y-W, Wong S-C, Abtahi M, Chen P. Electrospinning of polymer nanofibers: Effects on oriented morphology, structures and tensile properties. Composites Science and Technology. 2010;70:703–18. doi.org: 10.1016/j.compscitech.2010.01.010

[23] Pelipenko J, Kocbek P, Kristl J. Critical attributes of nanofibers: Preparation, drug loading, and tissue regeneration. International Journal of Pharmaceutics. 2015;484:57–74. doi.org: 10.1016/j.ijpharm.2015.02.043

[24] Torres-Martinez EJ, Cornejo Bravo JM, Serrano Medina A, Pérez González GL, Villarreal Gómez LJ. A Summary of Electrospun Nanofibers as Drug Delivery

System: Drugs Loaded and Biopolymers Used as Matrices. CDD. 2018;15:1360–74. doi.org: 10.2174/1567201815666180723114326

[25] Kim JH, Choung P-H, Kim IY, Lim KT, Son HM, Choung Y-H, *et al*. Electrospun nanofibers composed of poly(ε-caprolactone) and polyethylenimine for tissue engineering applications. Materials Science and Engineering: C. 2009;29:1725–31. doi.org: 10.1016/j.msec.2009.01.023

[26] Thakkar S, Misra M. Electrospun polymeric nanofibers: New horizons in drug delivery. European Journal of Pharmaceutical Sciences. 2017;107:148–67. doi.org: 10.1016/j.ejps.2017.07.001

[27] Kajdič S, Planinšek O, Gašperlin M, Kocbek P. Electrospun nanofibers for customized drug-delivery systems. Journal of Drug Delivery Science and Technology. 2019;51:672–81. doi.org: 10.1016/j.jddst.2019.03.038

[28] Yetisgin AA, Cetinel S, Zuvin M, Kosar A, Kutlu O. Therapeutic Nanoparticles and Their Targeted Delivery Applications. Molecules. 2020;25:2193. doi.org: 10.3390/molecules25092193

[29] Patra JK, Das G, Fraceto LF, Campos EVR, Rodriguez-Torres M del P, Acosta-Torres LS, *et al*. Nano based drug delivery systems: recent developments and future prospects. J Nanobiotechnol. 2018;16:71. doi.org: 10.1186/s12951-018-0392-8

[30] Barenholz Y (Chezy). Doxil® — The first FDA-approved nano-drug: Lessons learned. Journal of Controlled Release. 2012;160:117–34.doi.org: 10.1016/j.jconrel.2012.03.020

[31] Pepic I, Hafner A, Lovric J, Perina Lakos G. Nanotherapeutics in the EU: an overview on current state and future directions. IJN. 2014;1005. doi.org: 10.2147/IJN.S55359

[32] Tang F, Li L, Chen D. Mesoporous Silica Nanoparticles: Synthesis, Biocompatibility and Drug Delivery. Adv Mater. 2012;24:1504–34. doi.org: 10.1002/adma.201104763

[33] Wang Y, Zhao Q, Han N, Bai L, Li J, Liu J, *et al*. Mesoporous silica nanoparticles in drug delivery and biomedical applications. Nanomedicine: Nanotechnology, Biology and Medicine. 2015;11:313–27. doi.org: 10.1016/j.nano.2014.09.014

[34] Bitar A, Ahmad NM, Fessi H, Elaissari A. Silica-based nanoparticles for biomedical applications. Drug Discovery Today. 2012;17:1147–54. doi.org: 10.1016/j.drudis.2012.06.014

[35] Wu S-H, Hung Y, Mou C-Y. Mesoporous silica nanoparticles as nanocarriers. Chem Commun. 2011;47:9972. doi.org: 10.1039/c1cc11760b

[36] Zhou Y, Quan G, Wu Q, Zhang X, Niu B, Wu B, *et al.* Mesoporous silica nanoparticles for drug and gene delivery. Acta Pharmaceutica Sinica B. 2018;8:165–77. doi.org: 10.1016/j.apsb.2018.01.007

[37] Kwon S, Singh RK, Perez RA, Abou Neel EA, Kim H-W, Chrzanowski W. Silica-based mesoporous nanoparticles for controlled drug delivery. J Tissue Eng. 2013;4:204173141350335. doi.org: 10.1177/2041731413503357

[38] Haider A, Kwak S, Gupta KC, Kang I-K. Antibacterial Activity and Cytocompatibility of PLGA/CuO Hybrid Nanofiber Scaffolds Prepared by Electrospinning. Journal of Nanomaterials. 2015;2015:1–10.doi.org: 10.1155/2015/832762

[39] El-Aassar MR, Ibrahim OM, Fouda MMG, El-Beheri NG, Agwa MM. Wound healing of nanofiber comprising Polygalacturonic/Hyaluronic acid embedded silver nanoparticles: In-vitro and in-vivo studies. Carbohydrate Polymers. 2020;238:116175. doi.org: 10.1016/j.carbpol.2020.116175

[40] Sruthi R, Balagangadharan K, Selvamurugan N. Polycaprolactone/polyvinylpyrrolidone coaxial electrospun fibers containing veratric acid-loaded chitosan nanoparticles for bone regeneration. Colloids and Surfaces B: Biointerfaces. 2020;193:111110. doi.org: 10.1016/j.colsurfb.2020.111110

[41] Guarino V, Cruz-Maya I, Altobelli R, Abdul Khodir WK, Ambrosio L, Alvarez Pèrez MA, et al. Electrospun polycaprolactone nanofibres decorated by drug

loaded chitosan nano-reservoirs for antibacterial treatments. Nanotechnology. 2017;28:505103. doi.org: 10.1088/1361-6528/aa9542

[42] Xie Z, Paras CB, Weng H, Punnakitikashem P, Su L-C, Vu K, *et al.* Dual growth factor releasing multi-functional nanofibers for wound healing. Acta Biomaterialia. 2013;9:9351–9. doi.org: 10.1016/j.actbio.2013.07.030

[43] Zhou X, Chen L, Wang W, Jia Y, Chang A, Mo X, et al. Electrospun nanofibers incorporating self-decomposable silica nanoparticles as carriers for controlled delivery of anticancer drug. RSC Adv. 2015;5:65897–904. doi.org: 10.1039/C5RA11830A

[44] Wiltschka O, Böcking D, Miller L, Brenner RE, Sahlgren C, Lindén M. Preparation, characterization, and preliminary biocompatibility evaluation of particulate spin-coated mesoporous silica films. Microporous and Mesoporous Materials. 2014;188:203–9. doi.org: 10.1016/j.micromeso.2014.01.006

[45] Albarahmieh E, Albarahmieh M, Alkhalidi BA. Fabrication of Hierarchical Polymeric Thin Films by Spin Coating Toward Production of Amorphous Solid Dispersion for Buccal Drug Delivery System: Preparation, Characterization, and In Vitro Release Investigations. Journal of Pharmaceutical Sciences. 2018;107:3112–22. doi.org: 10.1016/j.xphs.2018.08.019

[46] Wang Q, Ye L, Wang L, Li P, Cao Y, Li Y. Rapid nanopatterning technique based on monolayer silica nanosphere close-packing by spin coating. Sci China Technol Sci. 2016;59:1573–80. doi.org: 10.1007/s11431-016-0316-2

[47] Esposito F, Cappabianca P, Fusco M, Cavallo LM, Bani GG, Biroli F, *et al.* Collagen-only biomatrix as a novel dural substitute. Clinical Neurology and Neurosurgery. 2008;110:343–51. doi.org: 10.1016/j.clineuro.2007.12.016

[48] Reina MA, López-García A, Dittmann M, de Andrés JA. Structural analysis of the thickness of human dura mater with scanning electron microscopy. Rev Esp Anestesiol Reanim. 1996;43:135–7.

[49] Goldschmidt E, Cacicedo M, Kornfeld S, Valinoti M, Ielpi M, Ajler PM, *et al.* Construction and in vitro testing of a cellulose dura mater graft. Neurological Research. 2016;38:25–31. doi.org: 10.1080/01616412.2015.1122263

[50] Suzuki Y, Iwaki M, Tani S, Oohashi G, Kamio M. Ion implantation into ePTFE for application of a dural substitute. Nuclear Instruments and Methods in Physics Research Section B: Beam Interactions with Materials and Atoms. 2003;206:538–42. doi.org: 10.1016/S0168-583X(03)00784-5

[51] Biroli F, Esposito F, Fusco M, Bani GG, Signorelli A, de Divitiis O, *et al.* Novel Equine Collagen-Only Dural Substitute. Operative Neurosurgery. 2008;62:ONSE273–4. doi.org: 10.1227/01.neu.0000317404.31336.69

[52] Malliti M, Page P, Gury C, Chomette E, Nataf F, Roux F-X. Comparison of Deep Wound Infection Rates Using a Synthetic Dural Substitute (Neuro-Patch) or Pericranium Graft for Dural Closure: A Clinical Review of 1 Year. Neurosurgery. 2004;54:599–604. doi.org: 10.1227/01.NEU.0000108640.45371.1A

[53] Ae R, Hamaguchi T, Nakamura Y, Yamada M, Tsukamoto T, Mizusawa H, *et al.* Update: Dura Mater Graft–Associated Creutzfeldt-Jakob Disease — Japan, 1975–2017. MMWR Morb Mortal Wkly Rep. 2018;67:274–8. doi.org: 10.15585/mmwr.mm6709a3

[54] MacEwan MR, Kovacs T, Osbun J, Ray WZ. Comparative analysis of a fully-synthetic nanofabricated dura substitute and bovine collagen dura substitute in a large animal model of dural repair. Interdisciplinary Neurosurgery. 2018;13:145–50. doi.org: 10.1016/j.inat.2018.05.001

[55] Mohtaram NK, Ko J, Agbay A, Rattray D, Neill PO, Rajwani A, *et al.* Development of a glial cell-derived neurotrophic factor-releasing artificial dura for neural tissue engineering applications. J Mater Chem B. 2015;3:7974–85. doi.org: 10.1039/C5TB00871A

[56] Esentürk İ, Erdal MS, Güngör S. Electrospinning method to produce drug-loaded nanofibers for topical/ transdermal drug delivery applications. İstanbul Üniversitesi Eczacılık Fakültesi Dergisi. 2016;46:49–69. doi.org:

[57] Elbialy NS, Aboushoushah SF, Sofi BF, Noorwali A. Multifunctional curcumin-loaded mesoporous silica nanoparticles for cancer chemoprevention and therapy. Microporous and Mesoporous Materials. 2020;291:109540. doi.org: 10.1016/j.micromeso.2019.06.002

[58] Chereddy KK, Coco R, Memvanga PB, Ucakar B, des Rieux A, Vandermeulen G, *et al.* Combined effect of PLGA and curcumin on wound healing activity. Journal of Controlled Release. 2013;171:208–15. doi.org: 10.1016/j.jconrel.2013.07.015

[59] Venkatasubbu GD, Anusuya T. Investigation on Curcumin nanocomposite for wound dressing. International Journal of Biological Macromolecules. 2017;98:366–78. doi.org: 10.1016/j.ijbiomac.2017.02.002

[60] Bollu VS, Barui AK, Mondal SK, Prashar S, Fajardo M, Briones D, *et al.* Curcumin-loaded silica-based mesoporous materials: Synthesis, characterization and cytotoxic properties against cancer cells. Materials Science and Engineering: C. 2016;63:393–410. doi.org: 10.1016/j.msec.2016.03.011

[61] Wang Y, Guo H, Ying D. Multilayer scaffold of electrospun PLA-PCL-collagen nanofibers as a dural substitute. J Biomed Mater Res. 2013;101:1359–66.

[62] Şen Karaman D, Gulin-Sarfraz T, Hedström G, Duchanoy A, Eklund P, Rosenholm JM. Rational evaluation of the utilization of PEG-PEI copolymers for the facilitation of silica nanoparticulate systems in biomedical applications. Journal of Colloid and Interface Science. 2014;418:300–10. doi.org: 10.1016/j.jcis.2013.11.080

[63] Moyer JR, Brown TH. Methods for whole-cell recording from visually preselected neurons of perirhinal cortex in brain slices from young and aging rats. Journal of Neuroscience Methods. 1998;86:35–54. doi.org: 10.1016/S0165-0270(98)00143-5

[64] Desai D, Karaman DS, Prabhakar N, Tadayon S, Duchanoy A, Toivola DM, et al. Design considerations for mesoporous silica nanoparticulate systems in facilitating biomedical applications. Open Material Sciences. 2014 doi.org:10.2478/mesbi-2014-0001

[65] Causey DH, Mays RP, Shamblee DA, Lo YS. A Practical Synthesis of Azetidine. Synthetic Communications. 1988;18:205–11. doi.org: 10.1080/00397918808077346

[66] Sarazen ML, Jones CW. Insights into Azetidine Polymerization for the Preparation of Poly(propylenimine)-Based CO_2 Adsorbents. Macromolecules. 2017;50:9135–43. doi.org: 10.1021/acs.macromol.7b02402

[67] Chaikittisilp W, Didas SA, Kim H-J, Jones CW. Vapor-Phase Transport as A Novel Route to Hyperbranched Polyamine-Oxide Hybrid Materials. Chem Mater. 2013;25:613–22. doi.org: 10.1021/cm303931q

[68] Patra D, Şen Karaman D, Desai D, El Khoury E, Rosenholm JM. Preparation of curcumin loaded mesoporous silica nanoparticles: Determining polarizability inside the mesopores. Materials Research Bulletin. 2016;84:267–72. doi.org: 10.1016/j.materresbull.2016.08.012

[69] Senthilkumar R, Karaman DŞ, Paul P, Björk EM, Odén M, Eriksson JE, *et al.* Targeted delivery of a novel anticancer compound anisomelic acid using chitosan-coated porous silica nanorods for enhancing the apoptotic effect. Biomater Sci. 2015;3:103–11. doi.org: 10.1039/C4BM00278D

[70] Roodbar Shojaei T, Hajalilou A, Tabatabaei M, Mobli H, Aghbashlo M. Characterization and Evaluation of Nanofiber Materials. In: Barhoum A, Bechelany M, Makhlouf ASH, editors. Handbook of Nanofibers Cham: Springer International Publishing; 2019 p. 491–522. doi.org:10.1007/978-3-319-53655-2_15

[71] Miller K, Hsu JE, Soslowsky LJ. Materials in Tendon and Ligament Repair. Comprehensive Biomaterials Elsevier; 2011 p. 257–79. doi.org: 10.1016/B978-0-08-055294-1.00218-X

[72] Chong LH, Lim MM, Sultana N. Fabrication and Evaluation of Polycaprolactone/Gelatin-Based Electrospun Nanofibers with Antibacterial Properties. Journal of Nanomaterials. 2015;2015:1–8. doi.org: 10.1155/2015/970542

[73] Mim ML, Sultana N. Comparison on in vitro degradation of polycaprolactone and polycaprolactone/gelatin nanofibrous scaffold. MJAS. 2017;21. doi.org: 10.17576/mjas-2017-2103-12

[74] Gordegir M, Oz S, Yezer I, Buhur M, Unal B, Demirkol DO. Cells-on-nanofibers: Effect of polyethyleneimine on hydrophobicity of poly-Ɛ-caprolacton electrospun nanofibers and immobilization of bacteria. Enzyme and Microbial Technology. 2019;126:24–31. doi.org: 10.1016/j.enzmictec.2019.03.002

[75] Amirian J, Sultana T, Joo GJ, Park C, Lee B-T. In vitro endothelial differentiation evaluation on polycaprolactone-methoxy polyethylene glycol electrospun membrane and fabrication of multilayered small-diameter hybrid vascular graft. J Biomater Appl. 2020;34:1395–408. doi.org: 10.1177/0885328220907775

[76] Niemczyk-Soczynska B, Gradys A, Sajkiewicz P. Hydrophilic Surface Functionalization of Electrospun Nanofibrous Scaffolds in Tissue Engineering. Polymers. 2020;12:2636. doi.org: 10.3390/polym12112636

[77] Wu J, Zhao C, Lin W, Hu R, Wang Q, Chen H, *et al.* Binding characteristics between polyethylene glycol (PEG) and proteins in aqueous solution. J Mater Chem B. 2014;2:2983. doi.org: 10.1039/c4tb00253a

[78] Wen S, Zheng F, Shen M, Shi X. Surface modification and PEGylation of branched polyethyleneimine for improved biocompatibility. J Appl Polym Sci. 2013;128:3807–13. doi.org: 10.1002/app.38444

[79] Danaei M, Dehghankhold M, Ataei S, Hasanzadeh Davarani F, Javanmard R, Dokhani A, *et al.* Impact of Particle Size and Polydispersity Index on the Clinical Applications of Lipidic Nanocarrier Systems. Pharmaceutics. 2018;10:57.doi.org: 10.3390/pharmaceutics10020057

[80] Beňová E, Zeleňák V, Halamová D, Almáši M, Petrul'ová V, Psotka M, *et al.* A drug delivery system based on switchable photo-controlled p-coumaric acid derivatives anchored on mesoporous silica. J Mater Chem B. 2017;5:817–25. doi.org: 10.1039/C6TB02040B

[81] Ziemba B, Franiak-Pietryga I, Pion M, Appelhans D, Muñoz-Fernández MÁ, Voit B, *et al.* Toxicity and proapoptotic activity of poly(propylene imine) glycodendrimers in vitro: Considering their contrary potential as biocompatible entity and drug molecule in cancer. International Journal of Pharmaceutics. 2014;461:391–402. doi.org: 10.1016/j.ijpharm.2013.12.011

[82] Ziemba B, Janaszewska A, Ciepluch K, Krotewicz M, Fogel WA, Appelhans D, *et al.* In vivo toxicity of poly(propyleneimine) dendrimers. J Biomed Mater Res. 2011;99A:261–8. doi.org: 10.1002/jbm.a.33196

[83] Najafi F, Salami-Kalajahi M, Roghani-Mamaqani H, Kahaie-Khosrowshahi A. Effect of grafting ratio of poly(propylene imine) dendrimer onto gold nanoparticles on the properties of colloidal hybrids, their DOX loading and release behavior and cytotoxicity. Colloids and Surfaces B: Biointerfaces. 2019;178:500–7. doi.org: 10.1016/j.colsurfb.2019.03.050

[84] Licciardello M, Ciardelli G, Tonda-Turo C. Biocompatible Electrospun Polycaprolactone-Polyaniline Scaffold Treated with Atmospheric Plasma to Improve Hydrophilicity. Bioengineering. 2021;8:24. doi.org: 10.3390/bioengineering8020024

[85] Zhu W, Castro NJ, Cheng X, Keidar M, Zhang LG. Cold Atmospheric Plasma Modified Electrospun Scaffolds with Embedded Microspheres for Improved Cartilage Regeneration. Li W-J, editor. PLoS ONE. 2015;10:e0134729. doi.org: 10.1371/journal.pone.0134729

[86] A R, Wf W, O G, M M, B G. Pcl/Peg Electrospun Fibers as Drug Carriers for the Controlled Delivery of Dipyridamole. J In Silico In Vitro Pharmacol.2015;01. doi.org: 10.21767/2469-6692.10003

[87] Quignard S, Coradin T, Powell JJ, Jugdaohsingh R. Silica nanoparticles as sources of silicic acid favoring wound healing in vitro. Colloids and Surfaces B: Biointerfaces. 2017;155:530–7. doi.org: 10.1016/j.colsurfb.2017.04.049

Appendices

Appendix A

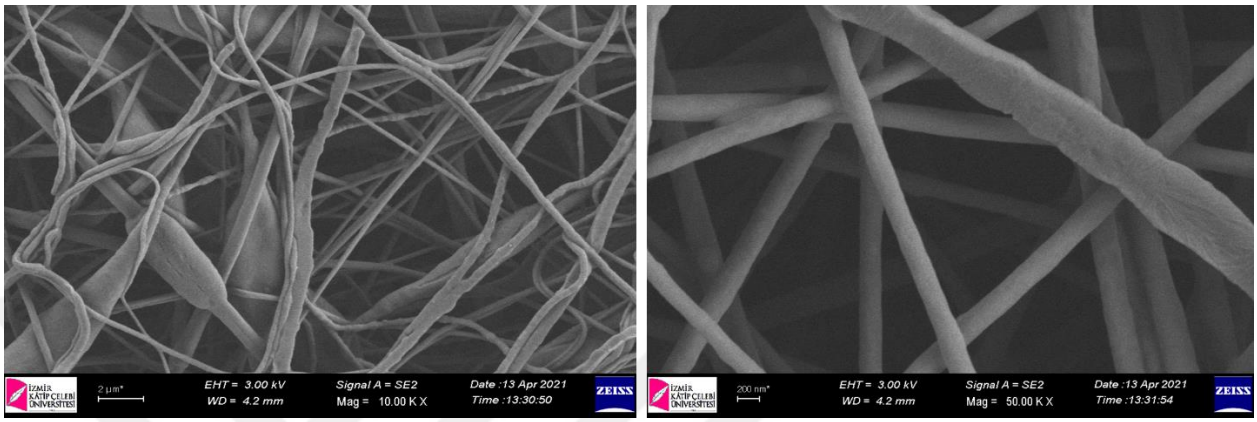

Appendix A: SEM images of NF100 after CAP treatment

Appendix B

Publications from the Thesis

Proceedings

1. 2021, EUROASIA SUMMIT 1st International Applied Sciences Congress, Development of Local Drug Delivery System for Tissue Regeneration

Journal Articles

1. 2021, Döndürmeli kaplama yöntemi ile kurkumin kaplanmış polikaprolakton nanolif yara örtülerinin hazırlanması ve *in vitro* etkinliğinin incelenmesi (Preparation Of Curcumin Spin-Coated Polycaprolactone Nanofiber Wound Dresses and investigation of *in vitro* Efficacy), European Journal of Science and Technology *(SUBMITTED)*

Projects

1. IKCU, İzmir Katip Çelebi University Scientific Project Coordination, Design of mesoporous silica nanocarrier integrated synthetic dura grafts and evaluation of their *in vitro* performances (Mezoporlu silika nanotaşıyıcı entegre edilmiş sentetik dura greft tasarımı ve *in vitro* etkinliğinin incelenmesi), Project no: 2020-ÖDL-MÜMF-0004

2. IKCU-İzmir Katip Çelebi University Scientific Project Coordination, Preparation of local drug delivery systems for tissue regeneration, (Doku rejenerasyonuna yönelik lokal ilaç iletim sistemlerinin hazırlanması), Project no: 2019-TYL-FEBE-0010

Curriculum Vitae

Name Surname : Nursu ERDOĞAN

Education:

2013–2018 İzmir Kâtip Çelebi University, Dept. of Biomedical Engineering

2018– İzmir Kâtip Çelebi University, Dept. of Biomedical Engineering/Master Program

Work Experience:

13-16 November 2017, Medica 2017, Düsseldorf-Germany

06.2017-07.2017, Mediracer, Oulu-Finland

07.2016-08.2016, Sayan Orthopedics, Izmir-Turkey, Internship

02.2016-06.2016, KOEK Biotechnology, Izmir-Turkey

Publications

1. 2021, Döndürmeli kaplama yöntemi ile kurkumin kaplanmış polikaprolakton nanolif yara örtülerinin hazırlanması ve *in vitro* etkinliğinin incelenmesi, European Journal of Science and Technology *(SUBMITTED)*

2. Coskun I., Erdogan N., Karaman Şen D., Karaman O.: Preparation of Serum Albumin Loaded Injectable Silica-Gel Matrix. Medical Technologies Congress (TIPTEKNO'19), October 3-5 2019, Kusadasi, Turkey, IEEE Xplore Digital Library

3. Onak G., Erdoğan N., Karaman O.: Effect of Different Number of Glutamic Acid Containing Peptide on Biomineralization and Cell Proliferation. Medical Technologies Congress (TIPTEKNO'18), November 8-10 2018, Gazi Magosa, KKTC
(Poster Presentation) & IEEE Xplore Digital Library
(DOI: 10.1109/TIPTEKNO.2018.8596830)

Proceedings

1. Karaman Şen D, **Erdogan** N.: Development of Local Drug Delivery System for Tissue Regeneration. EUROASIA SUMMIT 1st International Applied Sciences Congress, March 20-21, 2021, Georgia – Batumi, (Oral Presentation)

2. Onak G., Tatar A.G., Bilgili H.K., **Erdoğan N.**, Karaman O., Surface modification of aligned polycaprolactone nanofibers by different glutamic acid sequences containing peptides for enhanced biomineralization, The, 22. Biomedical Science and Technology Symposium (BIOMED 2017), May 12-14 2017, Ankara, Turkey, (Poster Presentation)

Projects and Funding

1.2019, TÜBİTAK 2210C National MSc/MA Scholarship Program in the Priority Fields in Science and Technology

2. IKCU, İzmir Katip Çelebi University Scientific Project Coordination, Design of mesoporous silica nanocarrier integrated synthetic dura grafts and evaluation of their *in vitro* performances Project no: 2020-ÖDL-MÜMF-0004

3. IKCU-İzmir Katip Çelebi University Scientific Project Coordination, Preparation of local drug delivery systems for tissue regeneration, Project no: 2019-TYL-FEBE-0010

4. 2016-1.Term, Effect of surface modification via peptide with different numerous glutamic acid sequences on nanofiber bio mineralization, cell retention and viability/ TÜBİTAK 2209-A Research Project Support Programme for Undergraduate Students